Part III: Lévy-dispersal kernels and dispersal ranges

7

Gap percolation and dispersal strategies in rainforests

7.1 Abstract

Rainforests biodiversity is sustained by the three-dimensional structure of their canopy which provides a wide range of physical microenvironments. Given the dynamic nature of the forest, the recognition of stable vertical layers or strata in the canopy is controversial. The spatial characterisation of potential habitats of understory species is not straightforward due to the complex structure of rainforest canopies and the wide ecological variability to which rainforest species can be adapted. Here we present a new description of potential understory habitats that give rise to a well-defined characteristic vertical scale of forest organization $h_c \approx 13m$. Species living in microenvironments occurring at canopy heights below this critical height h_c can only experience landscapes with disconnected habitat patches (i.e., fragmented habitat landscapes), while those species capable of living also above h_c will experience a fully connected landscape of suitable microenvironmental conditions. The possible implications for plant dispersal and animal colonisation strategies living at the understory or close-to-floor are discussed in relation to rainforest gap-dynamics, habitat loss and habitat fragmentation processes. Long-range and directed dispersal strategies (e.g., plant seed dispersal by animals) are optimal for those species living below h_c, providing the best exploration of scarce habitats and a major robustness to habitat changes. On the other hand, dispersal strategies of those species capable to exploit habitats above h_c need not to be based on

directed long-range mechanisms. Different dispersal strategies may in turn imply different sensitiveness of species to habitat loss and habitat fragmentation processes in the rainforest.

7.2 Introduction

Vertical organisation of trees and plants is a characteristic feature of rainforests. The so-called canopy structure provides the forest with a three-dimensional structural matrix where a wide range of community functions must be accomplished. Thus, the comprehension of canopy structure characteristics actually provides an appropriate framework to study the relationship between structure and function in ecosystems (Richards, 1952; Whitmore, 1997; Terborgh, 1992).

The canopy height variability of rainforests is a relevant descriptive factor of the changes in the quantity and quality of light determining microenvironment temperature, humidity, and soil moisture (Denslow, 1987; Becker et al., 1988). The structure of canopy heights has a very important role in shaping different microenvironments, that ultimately determine the threshold conditions that constraint plant growth and physiology (Zagt & Werger, 1996; Leigh, 1999), as well as physiological limits for many arboreal and terrestrial animals (Shelly, 1984; Leigh, 1999). These microenvironments strongly influence the competitive outcomes of different species living in the understory or the rainforest floor (Leigh & Wright, 1990; Reagan, 1992). Therefore, canopy height structure involves the three-dimensional organisation in space of a wide range of aboveground vegetation components (e.g trees, shrubs, herbaceous plants, lichens, fungi) and animal life forms (e.g., amphibians, small reptiles and mammals, arthropods and invertebrates) (Parker, 1995; Leigh, 1999). Overall, canopy height structure shapes and constrains the biodiversity of understory and close-to-floor species (Gilbert, 1980).

The traditional analysis of vertical forest architecture has been approached from the study of profile diagrams obtained from measurements of the trees in narrow strips of the forest (Richards, 1952; Terborgh, 1985). Since then, the vertical structure of forests is typically defined as layers or strata. The number of strata in rainforests is supposed to be greater than in temperate forests (Terborgh, 1985). Moreover, conceptual models exist to explain the organisation of canopy forests in strata (Terborgh, 1992). Nevertheless, strata are largely subjective and their exact demarcation is not obvious as the layers grade into each other. Recent techniques are making use of remote sensing analysis (such as laser altimetry) that

allows to obtain well-defined profiles based upon standardised measurements (Weishampel et al., 2001; Drake et al., 2002). The recognition, at different heights in the rainforest canopy, of different structures, species or environments to a degree that may define identifiable zones, is a useful aid to description or analysis but it has seldom received critical examination during decades (Smith, 1973; Baker & Wilson, 2000; Parker & Brown, 2000). Indeed, stratification can be considered a simplification and an abstraction given the dynamic nature of the forest. A forest is in a continuous state of flux, it consists of a mosaic of patches at all stages of the growth cycle (Whitmore, 1997). The dynamical changes in time and space of canopy gaps modify the intermingling of tree crowns in their search for light, therefore screening a possible stratified organisation of plant species. In this context, the existence of universal and robust properties in the vertical structure of rainforests is still an unresolved question.

These complementary perceptions of the structure of forest canopy (as vertically stratified or as a mosaic of growing gaps) give rise to a different spatial characterisation of understory species potential habitats. On the one hand, the 'static' vision is used to delimitate habitats in the vertical axis. Thus, emphasising the existence of specialist species adapted to live in certain canopy heights, as well as the existence of vertical competitive segregation processes of related species (Terborgh, 1992; Reagan & Waide, 1996). On the other hand, the 'dynamic' vision highlights the existence of strong relationships between understory species and certain growth cycle phases of the forest (i.e., gap-phase, building-phase, and mature-phase in Whitmore (1988)). Thus, potential habitats differentiation is based on the XY-plane dimension of the forest. The typical light-demandant and shade tolerant species distinction comes from such a dynamical envision of the rainforest canopy (Welden et al., 1991; Chesson & Pantastico-Caldas, 1994; Whitmore, 1997; Schnitzer & Carson, 2000; Molino & Sabatier, 2001).

However, the survival of many species in the understory depends on a great complexity of intertwined factors that must be sorted within a broad ecological or environmental range of conditions. Thus, although the life-history traits of some rainforest species may be related to a very specific set of ecological conditions, a wider range of survival conditions is also possible for many species. In particular, the possibility of covering a given range of conditions by some species might influence their survival on several growth cycle phases or on different vertical strata. In these cases, we need more realistic habitat characterisations based on the integration of the whole range of microenvironmental conditions in which the species is able to survive.

To understand how canopy structure is related to habitat availability in

species adapted to different ecological ranges (or microenvironmental conditions) we propose a new characterisation of rainforest understory habitats that integrates both previous envisions (i.e., static and dynamic) of rainforests. This characterisation of habitats takes into account the whole three-dimensional structure of vegetation by considering both the vertical layered structure on the Z axis, and the XY-plane mosaic structure itself. The habitat is defined as the whole set of microenvironments that exist below a maximum canopy height. The higher the maximum height, the wider the range of potential environmental conditions involved in the habitat. Thus, it is explicitly assumed: i) the capacity of many rainforest species to exploit different growth cycle phases as well as different canopy layers, and ii) the complex spatial pattern of understory microenvironments. Such a definition of habitat allows for the emergence of a well-defined critical height separating two domains in forest architecture. This critical height scale is obtained from the analysis of the spatial distribution of low canopy points (Welden et al., 1991; Condit, 1998) and reveals a threshold in the vertical organisation of the forest structure which is clearly related to the gap-dynamical aspects of the forest. The geometrical properties related to gap connectivity imposed by this threshold might have non-trivial consequences for dispersal or colonisation strategies of animals and plants within the understory or close to the forest floor. By means of a Lévy flight model the effect of a percolation threshold on dispersal strategies is illustrated.

7.3 Barro Colorado Island plot

We have used data on canopy height taken from the Barro Colorado Island (BCI) 50-ha plot (Hubble & Foster, 1986; Condit, 1998) that correspond to annual censuses of 5x5 meters resolution made from 1985 to 1993. Large forest plot research projects provide large sets of data collected using standardised techniques. The method used to estimate canopy height is specified in Hubble & Foster (1986) and Condit (1998). The canopy height data have already been used to map canopy gaps and their changes through time (Hubble & Foster, 1986) and as a way to assess light environment for saplings below (Welden et al., 1991). We have defined low-canopy points (LCP) as those sites where the maximum canopy height is lower than some given threshold (h). Thus, a different set of LCP ($\Omega(h)$) will be obtained using different threshold heights. For each chosen height, we get a set of canopy sites and a set of low-canopy sites (i.e., LCP). Low-canopy sites may be named also “gap” sites although we must understand a “gap” in

a broader sense than commonly used in rainforest studies. A set of gap sites may represent, in this case, a set of suitable patches conforming a three-dimensional habitat were a species can survive.

As an example, for arboreal species, low-canopy maps may define a threshold height below which a range of suitable understory habitats or environmental conditions are possible, involving both different strata and growth cycle phases. Moreover, canopy height is a good surrogate of the behaviour of canopy light transmittance from the top to the bottom of the canopy in spite of the fact that other structural factors of the canopy such as the spatial distribution of trees and foliage could provide a potential source of variability of the understory light levels (Pelt & Franklin, 2000). As a consequence, low-canopy maps (LCP spatial distribution) could also be shaping the landscape of potential available terrestrial microenvironments for some close-to-floor or terrestrial species (i.e., invertebrates and small vertebrates) strongly dependent on some light-related descriptors such as quantity and quality of light irradiance, temperature or humidity.

By progressively increasing the low-canopy cutoff by one-meter steps (from a minimum value of 1 m to the maximum value of 35 m height), 35 different low-canopy maps can be obtained representing habitat availability landscapes for different species. In Fig. 7.1 examples of LCP maps are shown for three different cutoff heights (h). Black cells represent suitable (available) habitat. White cells represent non-suitable habitat. As expected, the number of suitable patches $N_\omega(h)$ grows with h. The set of LCP grows in size and appears to be correlated in space: the new LCP that appear as h grows tend to be close to the previous ones.

7.4 Percolation in low-canopy maps

The analysis performed in this study involves the presence of a critical height at which canopy gaps percolate through the entire forest. Percolation is recognised as a key property in landscape ecology (Gardner et al., 1987; Turner et al., 2001). When some set of neighbouring, connected small-scale sites define a cluster spanning the entire system under consideration, such cluster is called a percolation cluster (Peitgen et al., 1992; Stauffer & Aharony, 1985; Milne et al., 1996; Keitt et al., 1997). Percolation phenomena influence metapopulation dynamics (Andrén, 1994; Bascompte & Solé, 1996; Wiens et al., 1997; With & King, 1999; Solé et al., 2004), invasion processes (Loehle et al., 1996; With, 2002), and are relevant to conservation biology (With, 1997; Bunn et al., 2000) and ecosystem function (Gamarra & Solé, 2002).

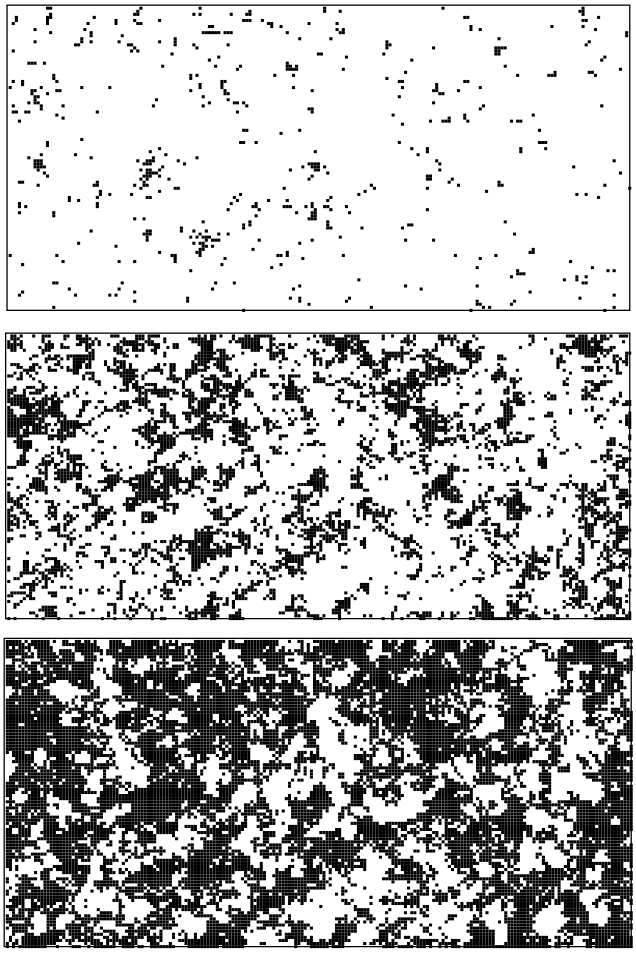

Figure 7.1: Low-canopy maps from Barro Colorado 50-Ha plot 1985 census data, see text. Here black cells are low-canopy points (LCPs) indicating suitable habitat. Non-suitable habitat is represented by white cells. LCPs are 5×5 m square sites such that their canopy is lower than some given threshold h. Here: Top $h = 5m$, Middle $h = 10m$ and Bottom $h = 15m$. Close to $h_c \approx 13m$ the set of LCPs becomes connected.

More precisely, let us consider the set of low-canopy points (LCP) $\Omega(h)$ that is defined for a given height h. For each h, a different set will be obtained. Fig. 7.2a shows the monotonic increase of $N_\omega(h)$, defined as the number of points in the set $\Omega(h)$) as h grows. However, the geometrical properties displayed by $\Omega(h)$ are far from monotonous. One key property is the emergence of percolation at $N_\omega(h_c)$ once a critical canopy height h_c is reached. A very useful characterisation of the transition to percolation in a lattice is provided by the computation of the time required for a "fire" to propagate through the system (Schroeder, 1991; Stauffer & Aharony, 1985). Let us assign an integer value $S(i,j) = 1$ to each LCP on $\Omega(h)$, and $S(i,j) = 0$ otherwise. A simple burning algorithm is defined as follows: (1) at step $t = 0$, the LCP at one edge of $\Omega(h)$ are burned, i.e., they take a new state $S(i,j) = 2$; (2) at the next step, those LCP that are nearest neighbours to burned sites are also burned. In this way, the fire propagates until no new LCP become burned (i.e., fire extinction) . The total time required to complete the fire spreading T_s (i.e., the time until fire extinction), is computed for different heights h. At percolation, $T_s(h)$ will present a maximum. For the BCI 50-ha plot the maximum $T_s(h)$ is reached at a height of $h \approx 13$ (Fig. 7.2b). The presence of a maximum and the overall profile obtained in Fig. 7.2b is easily understood in terms of the complexity of the underlying landscape. For $h < h_c$ the fire hardly spreads due to the fragmented nature of $\Omega(h)$, therefore fire extinction is rapid and $T_s(h)$ is low. For $h > h_c$, a more or less continuous set of connected gap sites is available with a rather homogeneous structure, and therefore, the time until fire extinction is large. Just at the transition $h \approx h_c$, the landscape $\Omega(h_c)$ is a fractal object (Solé, 2000) and the fire no longer propagates through a simple geometrical system. Instead, the percolation cluster displays complex features at multiple scales and the fire must follow such features over time. In a way, the transient time is tied to how difficult it is to describe the object. The divergence in $T_s(h_c)$ is characteristic of complex systems at the phase transition points (Peitgen et al., 1992; Solé, 2000).

In two-dimensional random uncorrelated landscapes, the spanning cluster of connected gaps would appear at a gap fraction $p_c \simeq 0.40725$ (Stauffer & Aharony, 1985). However, at the BCI 50-Ha plot, the largest cluster shows off at a somewhat greater gap fraction (see Fig. 7.2b). We simulated the fire spreading algorithm for both types of landscapes (i.e., the real BCI landscape and a random landscape with the same LCP). Above h_c, the landscape fractal dimension (box counting method) does not differ that of a purely random landscape ($D \approx 2$). Below it, fractal dimension gradually diminishes as gap sites become more sparse (Fig. 7.2c). The decrease in fractal dimension can also be explained in terms of strongest correla-

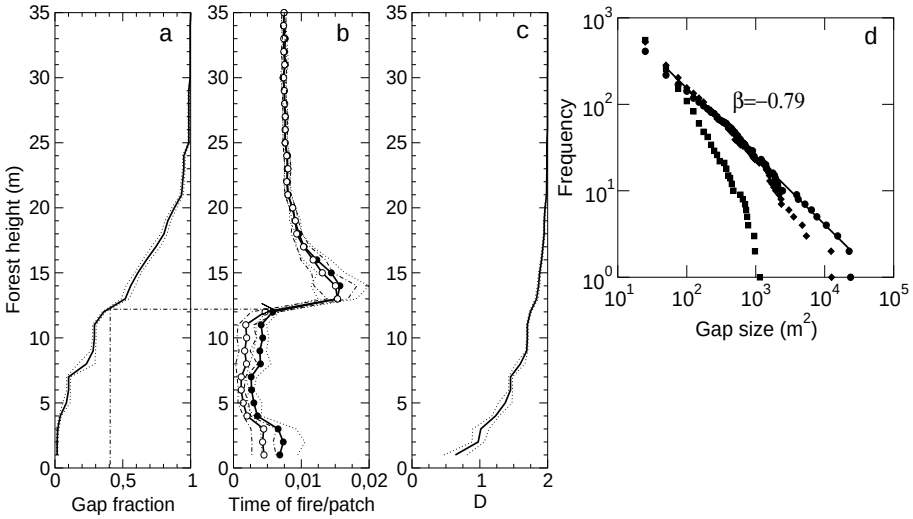

Figure 7.2: Percolation in the BCI plot, as measured from the burning algorithm. A maximum is reached at $h \approx 13m$, indicating that a percolation cluster is present. (a) Gap fraction in relation to forest height. Gap fraction is defined as the fraction of LCPs (or suitable sites) at every height (i.e., $N_\omega(h)/N_{total}$). Dashed lines indicate 95% confidence intervals for a series of eleven years (1985-1995). The arrow shows the height at which percolation should appear in a random landscape (lattice) under a Moore neighbourhood (8 nearest neighbours). In these type of lattices the critical value for the gap fraction is $p_c \simeq 0.40725$. (b) Fire lifetime ($T_s(h)$) in the burning algorithm. Black circles depict the results in the real landscape (1985 census data). White circles represent the results for 10 different random landscapes with the same number of LCPs. Dashed lines are confidence intervals for 10 different burning algorithms for every case. (c) Corresponding average fractal (box-counting) dimension plus confidence intervals for the whole 1985-1995 series. (d) Fractal behaviour close to the percolation threshold. The cumulative distribution of gap area sizes is shown for three different heights: $h = 8$ (squares), $h = 10$ (diamonds) and $h = 14$ (circles). As expected for a fractal, percolating cluster, a power law is obtained at $h \approx h_c$, i.e., $N_>(G) \approx G^{-\beta}$, with $\beta = 0.79 \pm 0.02$ and thus, $N(G) \approx G^{-\gamma}$ with $\gamma = \beta + 1 = 1.79$.

tions in gap spatial distribution below h_c. The strong spatial correlations between gap sites below h_c explain why $T_s(h)$ is higher than in random landscapes for $(h < h_c)$ (Fig. 7.2b). The differences between random and real BCI landscapes point to the greater importance of local connectivities close to the forest floor, due to greater spatial correlations.

At h_c, a very large cluster of connected LCP emerges, allowing for long-range correlations through all the landscape. Moreover, the distribution of gap area sizes in the percolation threshold is fractal, that is, no characteristic area sizes are identifiable. In Fig. 7.2d the cumulative distribution $N_>(G)$ is shown, defined as

$$N_>(G) = \int_G^\infty N(G)dG, \tag{7.1}$$

where $N(G)$ is the number of gaps of size G. The shape of this distribution changes with h, and actually reveals a scaling law

$$N(G) \approx G^{-\gamma} \cdot exp(G/G^*), \tag{7.2}$$

where G^* is a given (h-dependent) cutoff. Once $h = h_c$ is reached, a shift from a set of LCPs with a characteristic length scale to a scale-free (fractal) pattern is observed. The presence of a power-law is consistent with the existence of a percolation phase transition.

7.5 Dispersal strategies

Given the previous results, and in relation to species habitat availability, we aim to know the metapopulation consequences of the percolating geometry observed in rainforests architecture. The potential habitat availability for a species depends on two main factors: i) species biological constraints (i.e., physiological, behavioural or ecological) and ii) spatial and dynamical properties of the habitat. Within the biological constraints, both the species ecological ranges and their dispersal or colonisation strategies are of main importance in order to properly exploit the habitat (With & King, 1999). Thus, a good question to be answered is, how does habitat loss and fragmentation influence habitat availability in species with different ecological ranges and different dispersal strategies?

A Lévy flight model has been introduced to study the effect of dispersal or colonisation processes in different availability landscapes (i.e., low-canopy maps) by rainforest plants or animals living in the understory (arboreal) or close-to-floor (terrestrial). Lévy flights are random walks char-

acterised by the fact that the length of each successive steps or jumps l_j varies according to a power law function of the form:

$$P(l_j) = l_j^{-\mu} \tag{7.3}$$

with $1 < \mu \leq 3$. Values $\mu \leq 1$ do not correspond to normalisable probability distributions. Thus, a Lévy flight has no intrinsic jump length scale, and jumps of seemingly very long length may be observed. The power law exponent μ describing the jump length distribution is named Lévy exponent or Lévy index defininig a *continuum* of strategies from long-range to short-range dispersal. As the Lévy index increases from 1.1 to 3 extremely long jumps occur with less frequency, and thus a reduction in the overall dispersal scales is expected (from super-diffusive to gaussian macroscopic diffusion). In particular, for $\mu \geq 3$ typical Brownian dispersal strategy is recovered. Lévy flight patterns are common in large-scale animal movements (Viswanathan et al., 1999; Marell et al., 2002; Bartumeus et al., 2003), some of them inhabitants of the rainforests (Ramos-Fernández et al., 2004).

For each of the low-canopy maps obtained, different dispersal or colonisation strategies were simulated by changing the Lévy exponent of Lévy flight distribution from 1.1 to 3. Thus, the whole gradient from Lévy to Brownian strategies was covered. The results obtained are the same for both periodical and absorbent boundaries. The simulations proceed as follows: (1) An individual (or group of individuals) located in a suitable habitat is dispersed to another point of the landscape by randomly drawing a move or jump length from a Lévy flight distribution (i.e., truncated power-law with a range of jump lengths between 5 and 1000 m) (2) If the cell represents a suitable habitat, the species occupy the new habitat. If it is a non-suitable habitat or if it is an habitat already occupied, the individual (or group) is believed to be non viable in that cell and dies. (3) From the pool of habitats occupied (both old an new habitats included) an individual (or group) is chosen at random and a new dispersal/colonisation event is executed. (4) The simulation finishes when a certain dispersal effort has been made by the whole dispersing population. This dispersal effort is measured in terms of a total dispersal distance traversed by the population.

In particular, we define the dispersal efficiency function $\eta(\mu)$ to be the inverse of the total distance traversed by the population (i.e., the inverse of dispersal effort), so that:

$$\eta(\mu) = \frac{1}{< l > N} \tag{7.4}$$

where, N is the mean number of flights taken in a Lévy dispersal process

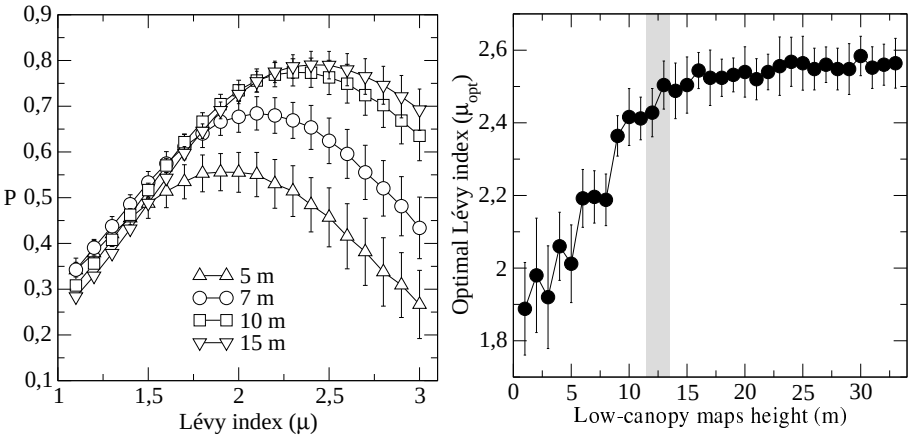

Figure 7.3: Left panel: Percentage of occupied landscape related to Lévy index exponent values (μ). Different low-canopy maps obtained at different heights (i.e., 5, 7, 10, and 15 m) show different optimal Lévy indexes. When higher cutoff heights are chosen, and thus, larger suitable habitat is being considered, higher is the optimal Lévy index. Right panel: A change from low to high optimal Lévy indexes (μ_o), i.e., large-range to short-range dispersal strategies, is observed as cutoff heights are increased from 1 to 35 meters. The asymptotic behaviour of this relationship is due to a percolation effect in the landscapes. Average and standard deviation values are computed from 25 curves obtained.

and $< l >$ is the mean dispersal-jump length of the process. Thus, dispersal efficiency is defined as in Viswanathan et al. (1999) but it is computed as a population dispersal efficiency and not as an individual searching efficiency. A low value of η can result from either a large N or a large $< l >$, corresponding to large and small μ, respectively. Small μ involves Lévy dispersal strategies based on few dispersal events but covering long dispersal distances, while large μ involves Brownian dispersal strategies that are based on a high number of local dispersal events. Thus, it is assumed that large-range dispersal involves higher time or energetic costs than short-range dispersal. Defining efficiency in such a way, and given a certain amount of time (or distance travelled), dispersal strategies based on Lévy distributions with small Lévy indexes (i.e., $\mu \leq 1.5$) provide a reduced *statistical* sampling power while those based on large Lévy indexes (i.e., $\mu \geq 2.5$) provide a reduced *spatial* sampling power. For any landscape, the optimal Lévy index will always be within the intermediate range $1.5 < \mu < 2.5$. However, a unique optimal μ value emerges for a specific landscape configuration.

For a given dispersal efficiency we compute the percentage of new occupied landscape as the ratio of the number of new occupied landscape

(i.e., number of suitable occupied cells previously non-occupied) to $N_w(h)$ (i.e., number of suitable cells). In Fig. 7.3, left different habitat suitability landscapes show different optimal Lévy indexes (μ). As higher cutoff heights are chosen to obtain the low-canopy maps (i.e., from 5 to 15 meters), higher is the optimal Lévy index. Fig. 7.3, right shows the optimal Lévy indexes (i.e., those indexes showing the maximum percentage of suitable habitat occupied provided certain dispersal effort) for each of the 35 low-canopy maps. As higher canopy cutoff heights are considered, more connected low-canopy maps are obtained, and a change from Lévy to Brownian dispersal strategies can be observed as we increase the cutoff height. An asymptotic behaviour related to the percolation effect is observed.

7.6 Discussion

Early studies of canopy structure suggested that the vertical organisation of canopy trees was layered and that some functional processes of rainforests should be dependent on this vertical layered structure (Richards, 1952). However, some authors have recently shown some limitations of 'classical' stratification studies in relation to scale dependence, point of reference and spatial averaging. They suggest that it may be more fruitful to discard the presumption of stratification entirely (Parker & Brown, 2000). However, it is the lack of objective quantitative measures that has prevented to rigorously define the presence of well-defined scales in rainforest spatial organisation.

In this study, we have shown that one of these possible scales can be described in terms of the percolation of canopy gaps once a critical canopy height (h_c) is reached. Indeed, when forests height-class distributions are complex (i.e., highly continuous distributions) this percolating critical canopy height (h_c) may provide useful structural and dynamical information about the forest. On the other hand, if height-class structure is simple (e.g., savannah forests) it may be better to identify the real strata (i.e., height classes) of the forest. Strictly speaking, the percolating critical canopy height (h_c) is a topological measure that only depends on the height-class structure of the forests. We have to look at the physical and dynamical factors providing a given height-class distribution to understand the emergence of a specific h_c. The most important factors involved in height-class distributions are density, gap-dynamics and external perturbances. In natural monospecific forests (i.e., single species forests with complex height-class distributions) this integrative measure may also provide comparable information on forest general status. Traditionally, the-

oretical analyses of gap-dynamics has been focused on the processes of gap formation and canopy recovery (Runkle, 1984; Solé & Manrubia, 1995; Kubo et al., 1996; Katori et al., 1998; Iwasa, 2000). However, these studies are typically restricted to gaps defined at some arbitrarily chosen height.

In an early study (involving the analysis of a single-height snapshot) the loss of spatial gap correlations at some given canopy height was explained in terms of tree fall dynamics (Solé & Manrubia, 1995). More recently, the influence of neighboring sites on transition rates (i.e. from non-gap to gap sites and viceversa) has been studied in detail (Schlicht & Iwasa, 2004; Satake et al., 2004). It is known that the rate of transition from a non-gap to a gap site increases with the number of neighbours that are currently in the gap state (Hubble & Foster, 1986; Kubo et al., 1996; Runkle, 1984; Kubo et al., 1996). This relationship may cause higher spatial correlations than expected from a pure random gap-formation process. However, the exact function relating the number of gap-state neighbours and the transition rates, as well as its possible dynamic consequences, have just started to be explored empirically and theoretically (Kubo et al., 1996; Schlicht & Iwasa, 2004; Satake et al., 2004).

Our results for the BCI rainforest, show that below h_c there exist higher correlations than the ones given in a pure random percolation process (where LCP would show a random distribution). This higher correlations disappear at $h > h_c$, consistently with a random-like distribution of crowns. Future models of gap-dynamics should take into account the presence of this critical height and the presence of non-random landscape correlations below the percolation height (h_c), providing a dynamical explanation for both.

The network of relationships established by rainforest species to survive may involve several spectra of microenvironments or growth cycle phases. Indeed, species are adapted to different ecological and environmental ranges. The understanding of biotic diversity begins with an understanding of the trade-offs that lead to specialisation. These trade-offs imply that "jack of all trades is master of none" (Leigh & Wright, 1990). An ecological *continuum* of strategies between those species adapted to very narrow and those adapted to very broad ecological ranges (i.e., specialists *vs.* generalists) exists. Within this *continuum*, the potentiality of exploiting habitats not only below the critical height h_c but also above, force very different ecological and evolutionary scenarios, in particular, for the optimisation of dispersal or colonisation rates in new available territory, either by increasing resource utilisation scale (O'Neill et al., 1988) or by using different movement strategies (With & King, 1999). The main assumptions involved in the dispersal model used to illustrate this fact, are: i)

Species habitat definition can integrate both different growth cycle phases (i.e. gap-dynamics stages) as well as different vertical microenvironments. Thus, low-canopy point maps can be related to habitat availability landscapes. ii) Strong habitat dependencies can be established for the survival of some species of the rainforests. iii) Random and local conditions trigger the ultimate dispersal process of the species. And iv) Extinction events are negligible once the species are settled in a suitable habitat, or similarly, the rates of colonisation are faster than those of extinction providing an always growing population. These conditions are general enough to cover a wide range of species living in the understory rainforest ecosystem.

Interestingly, the observed h_c is near 10 meters, which is the height chosen in field studies to differentiate low-canopy (light-demanding) from high-canopy (shade-tolerant) species (Welden et al., 1991). Low-canopy species able to survive in habitats that can only exist below h_c represent specialised species adapted to live in gap-light environments with high sun irradiance. Percolation theory predicts that in random percolating maps with a fraction of available habitat above a gap fraction of $p_c \approx 0.40725$, species can move freely through the landscape (O'Neill et al., 1988). However, in more aggregated landscapes (i.e., such as those below h_c in BCI) this value may increase because aggregation diminishes connectivity at long distances, and thus, more species can potentially coexist below h_c compared to a random landscape with the same $N_w(h)$.

Species with suitable habitats below h_c will always experience a strongly correlated and sparse landscape, and therefore may be very sensitive to landscape transformations involving both habitat loss and habitat fragmentation (i.e., loss of aggregation in spatial habitat distribution). Indeed, temporal fluctuations in gap formation and canopy recovery are much higher at lower heights in the forest. In such dynamic landscapes there is a lower survival probability in those species whose dispersal rate or, consequently, resource utilisation scale (O'Neill et al., 1988), are not large enough to overcome the changing structure of the landscape (Keymer et al., 2000; Johst et al., 2002). Therefore, strong evolutive pressures should exist to reinforce those mechanisms allowing the adaptation of dispersal strategies to a sparse and changeable underlying landscape. Thus, their dispersal strategies should be of the Lévy type (i.e., low Lévy indexes) and some plasticity should be necessary to adapt dispersal strategies to landscape changes. Colonisation of new available territory must involve few dispersal events but with large-distance coverage (i.e., long-distance dispersal allows the accessibility to far habitat aggregates). Moreover, directed dispersal strategies (e.g., animal seed dispersal) allows for a better adjustment of new habitat colonisation to a changeable

landscape. As an example, dispersal strategies of light-demanding plant species are commonly directed by animals (Leigh & Wright, 1990). Thus, below h_c, Lévy-type strategies based on directed mechanisms of dispersal should have a strong adaptive value. Species with such dispersal strategies should be more sensitive to habitat loss (which is already sparse) than to local habitat fragmentation.

On the other hand, species covering a sufficiently large range of environmental conditions providing some vertical microenvironments or some gap-dynamic stage with maximum canopy heights above h_c, will experience a fully connected landscape of potential suitable habitats through all the landscape. For example, shade-tolerant plant species (and associated fauna) capable of living in habitats not only below but also above h_c will experience a fully connected landscape. Two major consequences may be derived from this ecological situation: i) Long-distance dispersal and directed dispersal is not strictly necessary, and ii) Once in a connected landscape dispersal strategy doesn't need to be changed. Indeed, optimal dispersal strategies above h_c involve: i) a high number of short-scaled dispersal events (i.e., higher Lévy indexes than for species living in sparse landscapes (Fig. 7.3, left) and ii) independency from the underlying amount of available habitat in the landscape. The latter fact is explained becasue of a percolation effect. Although at increasing cuttoff heights the amount of available habitat increases, the dispersal strategy does not change. This is because optimal dispersal strategies mainly depend on the connectivity of habitat patches and not on the quantity of habitat. Once reached the percolation threshold, all the available habitat becomes connected, and this fact determines a unique dispersal strategy (i.e., a unique Lévy index) emerging as optimal for all the low-canopy maps above h_c (Fig. 7.3, right).

The evolutive costs of showing a greater physiological or behavioural plasticity (i.e., larger ranges of environmental conditions for survival) could be compensated by the fact that in fully connected landscapes, dispersal strategies should not necessarily be so efficient: short-distance and non-directed dispersal might be good enough to explore new territories. (e.g., dispersal strategies of shade-tolerant plant species are commonly driven by the wind (Leigh & Wright, 1990)). Generalist species have more available habitat by definition. Therefore, they should be less sensitive to habitat loss and habitat dynamical changes than highly specialized species. However, generalist species within a fully connected landscape could have evolved short-ranged and non-directed dispersal strategies and as a consequence could be much more sensitive to local fragmentation processes (i.e., loss of aggregation in spatial habitat distribution) when spreading to new territories.

Changes in the gap-dynamics of rainforests may modify the value of h_c and thus the relative potential number of species that are more sensitive to habitat loss (below h_c) or to fragmentation processes (above h_c), imposing important constrains to biodiversity patterns. Moreover, the presence of a critical height (h_c) may influence the competitive outcomes of closely related species. Competition between philogenetically related species (i.e., similar ecological ranges) can promote coexistence only when the less competitive one has evolved dispersal strategies capable to overcome its competitive disadvantage. That seems to be the case in the disjoint vertical distribution of lizards in Puerto Rico (Reagan, 1992; Leal et al., 1998). In such cases, the presence of a percolating critical height (h_c) should be decisive in the final competitive outcome. Once it is known h_c, some other practical consequences for rainforest biodiversity conservation could be derived. For example, the control of an invading species in the rainforest canopy should be managed in a very different way if their potential suitable habitats are all below h_c, or instead some of them are above.

We believe that a more integrative approach to the definition of rainforest species habitats, providing a more global and probabilistic approach to the study of the structure and functioning of rainforests, may be helpful to the understanding of some robust regularities at the whole system level. Such a new approach should allow us to establish new links between different components of the system (i.e., species, functional groups, etc.) or to compare different systems (i.e., rainforests) by means of objective measures. Moreover, we hope that this kind of approach may give further insights to the understanding of rainforest understory complexity by guiding new field studies, or integrating in a more general framework the already existent huge collection of case studies devoted to concrete rainforest species.

Acknowledgements

The authors thank Rick Condit for providing us with BCI data. We also thank David Alonso and William Parcher for useful discussions. This work has been supported by a grant PB97-0693 (JGPG) and by the Santa Fe Institute (RVS).

8

The role of the dispersal range in metapopulation dynamics

8.1 Abstract

Mobility and dispersal ability of individuals result in characteristic spatial patterns that influence metapopulation's persistence in a landscape. However, there is no clear understanding of how different dispersal capacities may modify extinction thresholds and transient dynamics of metapopulations in fragmented landscapes. On the one hand, mean field metapopulation models assume global dispersal across infinite landscapes. On the other hand, spatially explicit metapopulation models have focused in a rather limited number of dispersal strategies, although a wide range of dispersal capacities exist in natural populations. We have developed a spatially explicit model, and a pair approximation to the classical Levins metapopulation model, to study the effects of dispersal capacity (or range) on extinction thresholds and transient time behavior of metapopulations in relation to habitat loss. We outline three closed-form analytical solutions. The first one for the transient time duration of metapopulations when mean-field assumptions are appropriate. The second one expresses equilibrium patch occupancy in terms of metapopulation parameters (i.e., extinction and colonization rates), habitat loss and dispersal range. And the third one relates critical habitat destruction values for metapopulation extinction to metapopulation parameters and dispersal ranges. Furthermore, our results are accompanied with exact stochastic realizations of the analytical model proposed in a spatially explicit system. The results of

the new model show that: i) increasingly localized dispersal ranges shifts the extinction thresholds to lower values of habitat loss, ii) transient times are larger for increasingly localized dispersal ranges and diverge near the corresponding extinction thresholds, and iii) landscape fragmentation and habitat destruction impinge in metapopulation colonization rates through their negative effects within the dispersal range.

8.2 Introduction

Habitat loss is widely considered to be the present principal threat to the long-term survival of species both locally and worldwide (Andrén, 1994; Barbault & Sastrapradja, 1995). Furthermore, habitat fragmentation by human beings is increasing at an alarming rate in many habitats around the world and has been shown to have detrimental effects on genetic diversity, population survival and ecosystems structure and function (Forman, 1995; Fahrig, 2002, 2003). Years after its introduction by Levins (1969, 1970), metapopulation theory has been recognized as one of the current paradigms for the conservation of spatially structured populations in fragmented landscapes (Hanski & Simberloff, 1997).

The current population ecological theory on habitat loss and fragmentation is largely based on Lande (1987) extension of Levins model (Levins, 1969). These simple analytical models are based on differential or difference equations that assume homogeneous couplings between entities with no explicit spatial structure or other types of heterogeneities. Such spatially implicit models, named **mean field** models (Levin & Durret, 1996) are adequate to formalize and synthesize the essential mechanisms driving a given population dynamics in a simple and analytically tractable way. However, they are unsuitable for understanding the dynamical processes that occur in spatially heterogeneous environments (Bascompte, 2001). For example, if the mobility and dispersal ability of individuals are limited, ecological and demographic processes will result in characteristic spatial patterns in which individuals of the same type tend to form clumps. These clumps cause population phenomena that are qualitatively different from those expected in well-mixed systems (i.e., mean field approximation) and can affect species coexistence, invasion, evolution, and species or genetic diversity (Sato & Iwasa, 2000). An alternative to the shortcomings of mean field models are **spatially explicit models** such as lattice models (Bascompte & Solé, 1996; Hiebeler, 1997; Bascompte & Solé, 1998; Pascual & Guichard, 2005).

Spatially explicit (lattice) models of metapopulations have shown that

landscape structure and landscape patch dynamics, can strongly affect metapopulation dynamics and persistence (Bascompte & Solé, 1996; Bevers & Flather, 1999), the outcome of species interaction (Dytham, 1994; Tilman et al., 1994; Dytham, 1995; Tilman & Kareiva, 1997), and the behavior of territorial populations (Lande, 1987). Usually the effects are highly nonlinear, associated with the existence of critical thresholds determined by the structural properties of the landscape and the demographic properties of the metapopulation. In particular, spatial models predict the existence of "extinction thresholds" in relation to habitat loss and fragmentation (Hanski et al., 1996). An extinction threshold is defined as the minimum amount of habitat required for a population of a particular species to persist in a landscape (Lande, 1987; Lawton et al., 1994; Hanski et al., 1996). Commonly, spatially explicit metapopulation models are equivalent to *contact processes* (Mollison, 1977; Snyder & Nisbet, 2000), where an empty patch is colonized only from its nearest-neighbor patches. In such cases, lower extinction thresholds are expected than in spatially implicit models (i.e., Levins model), suggesting that when dispersal is rather limited, more habitat is required for population persistence (Adler & Nuernberger, 1994; Bascompte & Solé, 1996; Hill & Caswell, 1999; With & King, 1999b). However, a wide variety of dispersal strategies and dispersal ranges exist in nature (Bullock et al., 2002). An important gap of knowledge in metapopulation theory is related to understanding how this diversity in dispersal capacities modify the persistence of metapopulations in fragmented landscapes.

The purpose of the present study was to elucidate the effects of habitat loss and fragmentation on spatially structured metapopulations with different dispersal capacities. In our model, dispersal capacity is represented as a dispersal range or domain (i.e., a subset of landscape over which species can be dispersed). There are many empirical measures such as mean dispersal distance, maximum dispersal range, dispersal area, etc. that can be directly related to the dispersal parameter of the model. Our approach is based on spatially explicit (lattice) metapopulation modeling and on pair approximation methodology. The pair approximation is a technique originally developed in the physical sciences to correct mean field models, such as the classical Levins model, when the explicit spatial structure should not be ignored (Dickman, 1986; Katori & Konno, 1991). Pair approximation was introduced in ecology and epidemiology as a way of exploring spatial structure in the contact process and in similar spatially explicit models (Matsuda et al., 1992; Harada & Iwasa, 1994; Sato et al., 1994; Satulovky & Tomé, 1994; Harada et al., 1995). Subsequently the applications of pair approximation and other moment closure techniques in ecology have quickly in-

creased (Sato & Konno, 1995; Kubo et al., 1996; Levin & Durret, 1996; Nakamaru et al., 1997; Takenaka et al., 1997; Pacala & Levin, 1997; Iwasa et al., 1998; Nakamaru et al., 1998; Levin, 1998; Ives et al., 1998; Bolker & Pacala, 1999; Dieckmann et al., 2000; Hiebeler, 2000). Pair approximation has recently been used to analyze the spatial structure of habitat loss in metapopulation dynamics for both discrete-time (Hiebeler, 2000), and continuous-time models (Ovaskainen & Hanski, 2002). However, this method has never been used to explore the effects of dispersal capacity on metapopulation extinction thresholds and dynamics, in fragmented landscapes. Our goal is to present an improved general understanding of how dispersal capacity modifies metapopulation dynamics by providing: i) new analytical solutions of an extended version of the classical Levins model which includes both habitat destruction and dispersal ranges, and ii) exact stochastic realizations of a spatially explicit version of the model analyzed.

8.3 The classical Levins metapopulation model

A metapopulation can be defined as a set of geographically distinct local populations maintained by a dynamical balance between colonization and extinction events. The simplest, first approximation to metapopulation's concept is formalized by the model of Levins (Levins, 1969), which captures the dynamics of a metapopulation:

$$\frac{dp}{dt} = cp(1-p) - ep, \tag{8.1}$$

where p is the fraction of patches occupied (*occupancy*), and c and e are the colonization and extinction rates, respectively.

Thus, Levins expressed this balance as a simple differential equation with no details on the spatial structure or other types of heterogeneities, and thus belongs to the class of mean field theories (Levin & Durret, 1996; Bascompte, 2001). The model assumes constant and uniform patch quality (i.e., any patch is equally available for colonization by the species under study and populations inhabiting every patch experience an equal extinction risk. In spite of its unrealistic assumptions, it provides several critical insights into metapopulation dynamics. First, since the only non-zero stable stationary state of Eq. 8.1 is given by $p^* = 1 - \frac{e}{c}$, a very simple rule for metapopulation persistence can be obtained: colonization must be greater than extinction rate (i.e., $c > e$). And second, it predicts that equilibrium metapopulations will never occupy all patches.

Following Lande (1987, 1988) one can easily introduce habitat loss into the framework of Levins model (8.1). If a fraction D of sites are perma-

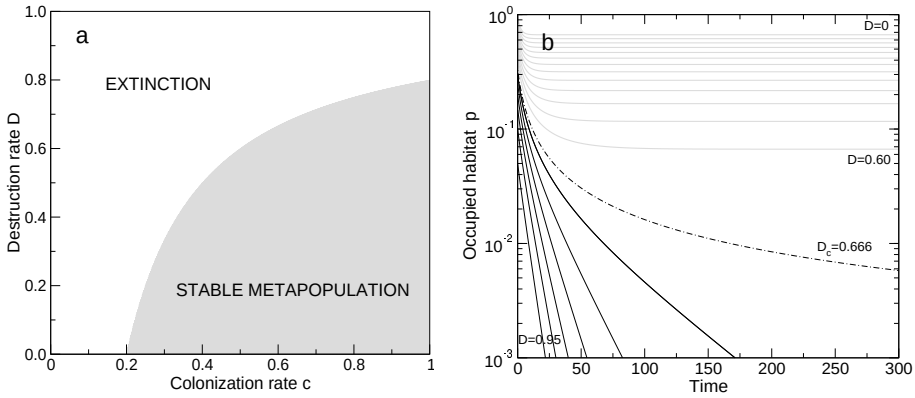

Figure 8.1: (a) Parameter space for the Levin's model using a local extinction rate $e = 0.2$. Two domains are obtained from the transition curve $D_c = 1 - e/c$ (see text). This critical boundary separates the domain where a stable metapopulation exists from the extinction phase, where no metapopulation is able to persist. (b) Habitat occupancy predicted by the Levins model ($c = 0.6$, $e = 0.2$) in relation to time for different degrees of habitat loss (D). As habitat destruction increases metapopulation equilibrium values decay through time.

nently destroyed, this reduces the fraction of vacant sites that can potentially be occupied. Eq. 8.1 becomes:

$$\frac{dp}{dt} = cp(1 - D - p) - ep. \tag{8.2}$$

and therefore, the combined effects of demographic parameters and habitat loss can be analyzed.

8.3.1 Stationary states

Eq. 8.2 has two equilibrium points (to be obtained from $dp/dt = 0$): $p^* = 0$ (extinct population) and

$$p^* = 1 - D - \frac{e}{c}. \tag{8.3}$$

The two points match through the curve $1 - D - e/c = 0$, which gives a critical destruction level D_c associated to extinction-colonization rates:

$$D_c = 1 - \frac{e}{c}. \tag{8.4}$$

Once we cross this threshold (i.e., if $D > D_c$) the population gets inevitably extinct. This situation is illustrated in (Fig. 8.1a). Here the critical line separates the two qualitative types of metapopulation allowed. Essentially, as we approach the critical value D_c by increasing the amount

of habitat destroyed, the frequency of populated patches decays linearly (Fig. 8.1b) . This frequency becomes zero at the boundary.

The main lesson to be extracted from this model is that (perhaps against our intuition) no sustainable metapopulation is possible once we reach a critical amount of habitat loss, in spite that a fraction of $1 - D$ patches is still habitable. The interaction between available areas and demographic parameters (here reduced to two local, average rates) establishes an extinction threshold for habitat loss known as the Levins rule (Lande, 1987; Hanski et al., 1996). As can be seen from Eq. 8.4, the interaction between D_c and e for a fixed c is linear, whereas D_c changes in a nonlinear way with c (for a fixed e).

8.3.2 Transient dynamics

Transient time in population dynamics refers to the time it takes for a population to return to population-dynamic equilibrium (or close to it) following a perturbation in the environment or in population size. Depending on the direction of the perturbation, transient time may either denote the time until extinction (or until the population has decreased to a lower equilibrium level), or the recovery time needed to reach a higher equilibrium level (Ovaskainen & Hanski, 2002). An additional information can be obtained by looking at the delay time until the steady state is reached. Specifically, let us consider a very small initial population $p_0 \ll 1$ and the time required to reach the steady state p^*. The approach to the equilibrium state takes place in a sigmoidal way: solving the equation for the Levins model we have:

$$p(t, D) = \frac{p_0 \Gamma}{p_0 + (\Gamma - p_0) \exp(-c\Gamma t)}, \tag{8.5}$$

where $\Gamma = 1 - D - e/c$ and therefore $\Gamma = p^*$. How fast this approach occurs can be computed by using the time $T(D, \eta)$ required to reach a fraction $p = |p^* - \eta|$ of the steady population, where η is considered a small perturbation from the steady state (i.e., $\eta \ll \Gamma$). It can be shown that for $D \leq D_c$ such delay time is given by (see Appendix 8.8.1)

$$T(D, \eta) = \frac{1}{c\Gamma} \ln \left[\frac{\Gamma - \eta}{p_0} \left(\frac{\Gamma - p_0}{\eta} \right) \right]. \tag{8.6}$$

And for $D > D_c$ such delay time $T(D, \eta)$ is given by

$$T(D, \eta) = \frac{1}{\Omega} \ln \left(\frac{\eta}{p_0} \right), \tag{8.7}$$

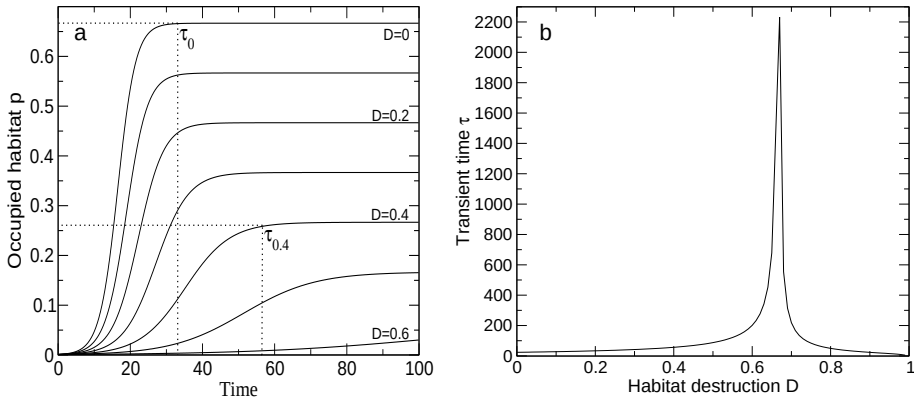

Figure 8.2: (a) The Levins model ($c = 0.6$, $e = 0.2$) predicts lower equilibrium values and greater transient times (τ) as habitat loss increases. The transient time is the time it takes for a population to reach population-dynamic equilibrium (or close equilibrium values). (b) Transient time behavior of the Levins model ($c = 0.6$, $e = 0.2$) in relation to habitat loss (D). A divergence is obtained near the critical threshold $D_c = 0.66$. For $D > D_c$ a quick decay takes place, whereas the behavior for $D < D_c$ is highly nonlinear: a divergence actually occurs close to D_c indicating that the time required in order to colonize the available habitat until reaching $p = \eta(1 - D - e/c)$ rapidly increases. Results obtained from equations 8.6 and 8.7 for $D \leq D_c$ and $D > D_c$ respectively. In this case we have used $p_0 = 0.001$ and $\eta = 0.95$.

where $\Omega = c(1 - D) - e$. As we can easily check in Fig. 8.2, this delay time involves a discontinuous change (or singularity) for $D = D_c$. One important consequence of this result is that the time required to colonize available habitat sharply increases as we approach the critical destruction level. This means that a given seed population will be not just small, but rather slow in spreading through available patches. One prediction from this observation is that, under stochastic factors such as finite population size and environmental perturbations, the likelihood of extinction would actually increase rapidly even at some distance from the critical threshold.

8.4 A spatial explicit model with dispersal

A simple and useful method for modeling population and evolutionary dynamics in a spatially explicit way is to use a lattice, or cellular automaton, model (Durrett & Levin, 1994; Dieckmann et al., 2000). An advantage of lattice models over traditional population dynamic models that are merely based on population densities or abundances is the ease and flexibility with which ecological interactions occurring between nearby individuals can be incorporated. In this respect, lattice models are closely related

to a group of models called “individual-based models” (Judson, 1994) or “agent-based models” (Axelrod, 1997). In the field of applied mathematics and theoretical physics, lattice models are called “interacting particle systems” (Liggett, 1985; Levin & Durret, 1996). Finally, lattice models have the advantage of explicitly considering stochasticity caused by finite numbers of individuals (discreteness), so called demographic stochasticity in population ecology and random drift in population genetics. Such stochasticity is often neglected in traditional models of differential equations in theoretical ecology (Sato & Iwasa, 2000).

To study the dynamic consequences of dispersal capacity among local populations (on equilibrium steady states and transient times) we introduce a spatially explicit metapopulation model with local colonization from neighboring sites. The model is based on the following assumptions:

- *Uniform lattice*: The metapopulation is established in a lattice-structured habitat. Each patch occupies one site of the lattice. Thus, each lattice site is either occupied by a population $[+]$ or empty $[0]$. The lattice can be one-dimensional (linear) or two-dimensional (square, triangular or hexagonal). We assume that the lattice space is infinitely large, homogeneous and isotropic. All lattice sites have the same number of nearest neighbors.

- *Random destruction*: From the very first beginning a given percentage of the total lattice sites are destroyed. These sites are not recovered and can not be colonized. Thus, destruction is a static parameter.

- *Extinction*: Each occupied patch can become empty at a constant extinction rate (e), which is defined as the expected number of death events in a unit time interval resulting in a transition from + to 0. The death rate at a site is independent of the state of neighboring sites.

- *Colonization*: Each empty site can be colonized from a set of neighboring sites (z) within a given *dispersal range* or *domain* at a given constant rate. The colonization rate per each neighboring patch is a constant defined as c/z. Thus, the colonization rate c is the maximum colonization rate into an empty patch, which is realized when all the neighbors in the dispersal range are occupied. An empty site will be filled by a local population at a rate proportional to the number of occupied neighbors in the dispersal range.

Thus, the dispersal range of a given patch Δ can be defined as the set of equivalent potential colonizer patches in its neighborhood. Specifically, we

define the dispersal range Δ as a square centered at the empty patch to be colonized with a maximum side length (l_{max}, maximal dispersal distance) so that $l_{max} \leq L$, where L is the one-dimensional size of the whole system. In a regular square lattice the relationship between the number of neighbors (ocuppied and available) z, and l_{max} is: $z = (2l_{max} + 1)^2 - 1$. Both z (dispersal range or domain) and l_{max} (maximal dispersal distance) are indicators of the dispersal capacity of the metapopulation. When Δ involves all the patches in the lattice, we obtain a spatially *implicit* model equivalent to the mean-field model (for large enough lattices). In a spatially *implicit* model, such as Levins model, it is assumed that each cell (representing an individual, patch population, etc.) can interact with all the rest of the cells conforming the lattice, thus representing well-mixed metapopulations. It is assumed that the size of the dispersal range does not depend on the location of the empty patch. Moreover, within the dispersal range, all the occupied patches contribute equally to the overall colonization pressure on the central free site. Therefore, no *contact distributions* (Mollison, 1977) or *dispersal functions* (Minogue, 1986) are assumed within Δ.

The basic dynamical, local processes can be illustrated as follows:

$$\text{Extinction: } [+] \xrightarrow{e} [0] \tag{8.8}$$

$$\text{Colonization: } [+,0] \xrightarrow{c/z} [+,+] \tag{8.9}$$

where $[+-0]$ indicates a pair of neighbors where one of the two sites (in this case the right hand one) undergoes a transition. Note that an empty site cannot be colonized unless a neighboring site from the dispersal range is occupied. For a given dispersal range, this constraint causes *density-dependent* colonization, where the colonization rate is proportional to the number of occupied potential colonizers. However, when considering different dispersal ranges we have to be aware of the fact that for any dispersal range (any set of neighboring sites z) the maximum colonization rate will be c. This means that the contribution of a neighboring patch to the overall dispersal range colonization pressure decreases as the dispersal range increases. In this sense, the spatially explicit Levins model involves a *frequency-dependent* colonization, that is, colonization depends on the fraction of occupied neighboring sites in the dispersal range but not on the absolute number of occupied sites.

8.5 Exact stochastic simulations: spatially implicit model

There are two formalisms for mathematically describing the time behavior of a spatially extended system. The *deterministic* approach regards the time evolution as a continuous, wholly predictable process which is governed by one or a set of coupled ordinary differential equations; the *stochastic approach* regards the time evolution as a kind of random-walk process which is governed by a single differential-difference equation: the "master equation" (van Kampen, 1992; Gillespie, 1977). Stochastic versions of the Levins' model and Levins-like models have been studied (Gurney & Nisbet, 1978; Etienne & Nagelkerke, 2002; Alonso & McKane, 2002; Alonso, 2003), but unfortunately, the stochastic master equation is often mathematically intractable. There is, however, a way to make exact numerical simulations within the framework of the stochastic formulation without having to deal with the master equation directly. Exact stochastic numerical simulations are based on the "stochastic simulation algorithm", created by Gillespie (1976, 1977, 1992) for studying coupled chemical reactions. The stochastic algorithm has been already improved and used successfully in metapopulation spatial explicit simulations (Alonso & McKane, 2002; Alonso, 2003). This algorithm is particularly useful when the master equation is mathematically intractable or when modeling transient dynamics of stochastic systems. The stochastic simulation algorithm and the general simulation procedure used is explained in detail in Appendix 8.8.2 (see also Technical Appendix D).

By following the simulation strategy of Appendix 8.8.2 we test the accuracy of exact stochastic simulations based on a spatially *implicit* model (i.e., well-mixed metapopulations) and compare them with the analytical solutions obtained for the mean-field model. The system is modeled as a continuous-time, single-step Markov process where transitions occur asynchronously so that within a short enough time interval only a single transition can take place. To obtain the equilibrium occupancy values for each habitat loss level, the metapopulation started with an arbitrary low fraction of occupied sites (randomly scattered in the lattice), and let the system evolve toward a stationary probability of occupancy. We have also computed the exact transient times until reaching an occupancy probability very near the equilibrium value. Figure 8.3 shows the results obtained from the mean field approximation and the exact stochastic spatially implicit simulations of the Levins model with destruction. A very good agreement is found for both stationary states and transient dynamics.

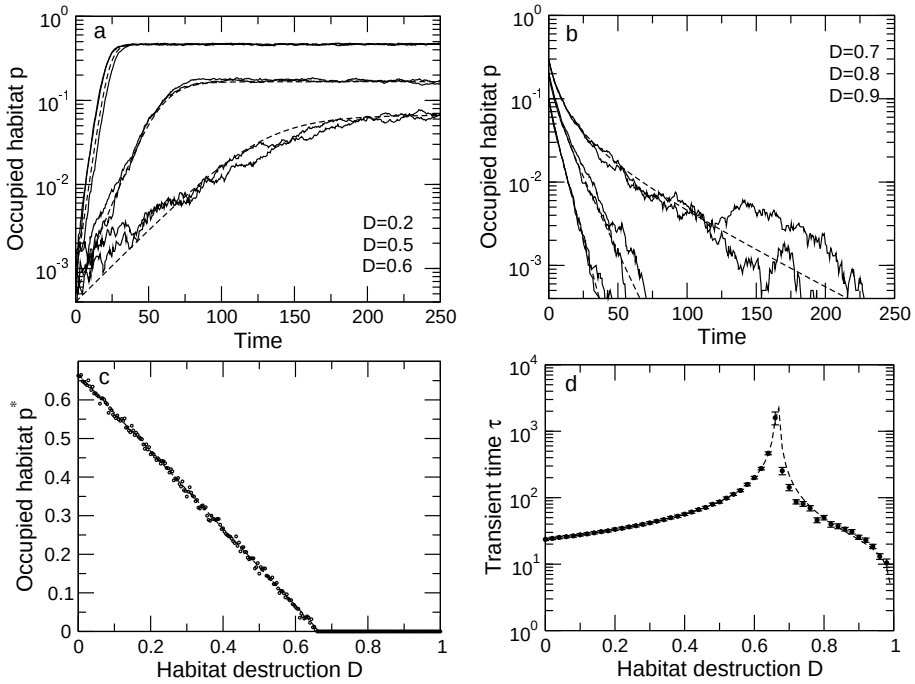

Figure 8.3: Stochastic exact realizations in comparison with numerical integrations of the Levins' model equation ($c = 0.6$, $e = 0.2$ therefore $D_c = 0.666$). Two stochastic exact realizations are shown for each numerical integration. (a) For $D < D_c$, and (b) for $D > D_c$. All simulations were run in a 100×100 lattice and a starting ocuppancy value of $p_0 = 0.001$ in (a) and $p_0 = 1 - D$ in (b). (c) Comparison between the analytical equilibrium value equation $p = 1 - D - e/c$ and exact stochastic realizations (lattice 100×100). (d) Comparison of the results obtained from the analytical approximation (equations 8.6 and 8.7) in solid line, and from the spatially explicit and stochastic Levins model (dots with standard deviation bars). Simulations were run on a 512×512 lattice. For each D value, results were obtained by averaging 25 individual stochastic realizations. The parameter values chosen are $c = 0.6$, $e = 0.2$, $\eta = 0.05$ and $p_0 = 0.001$.

8.6 A pair approximation

A major problem of spatially explicit models, whether lattice models or models based on continuous space, is that analysis is often restricted to direct computer simulation. Mean field approximation, which neglects spatial structures by assuming complete mixing of individuals, often shows behavior that is qualitatively different from that observed in direct computer simulations (Dieckmann et al., 2000). Fortunately, there is a useful method for analyzing lattice models and diminishing the discrepancy between mean field and explicit simulations. This method was introduced by Matsuda in an analysis of the evolution of social interaction in lattice-structured populations (Matsuda, 1987; Matsuda et al., 1987). Since then, the pair approximation method has been widely applied (Matsuda et al., 1992; Harada & Iwasa, 1994; Harada et al., 1995; Levin & Durret, 1996; Levin, 1998; Ives et al., 1998; Iwasa, 2000) and improved (Sato et al., 1994; Ellner, 2001).

The importance of considering correlations between interacting individuals has already been pointed out, for example in the case of insect population dynamics (Ives & May, 1985), where a spatially clumped distribution creates a conditional density in the neighborhood of an individual much higher than the density from random samples. This method consists in constructing a closed dynamical system comprising two components: first, the overall densities of lattice sites in specified states and, second, the conditional probability that a randomly sampled nearest neighbor of a site is in a specified state. Pair approximation is a kind of decoupling approximation, developed in statistical physics, also referred to as a "moment closure method" (Sato & Iwasa, 2000). The pair approximation treats the degrees of spatial clumping as a separate dynamic variable rather than as a given parameter, since the degree of clumping and nearest-neighbor correlation are also the result of demographic processes and ecological interactions (Harada & Iwasa, 1994).

The spatially explicit model with dispersal ranges (expressed in terms of the number of neighbors z of a given patch) can be described by the pair approximation method in terms of the following system of equations (see Appendix 8.8.3 and (Sato & Iwasa, 2000)):

$$\begin{aligned}
&\frac{d\rho_+}{dt} = -e\rho_+ + c(1-D-q_{+/+})\rho_+ \\
&\frac{dq_{+/+}}{dt} = -q_{+/+}[c(1-D-q_{+/+}) - e] + \\
&+2\left\{-eq_{+/+} + c\left[\frac{1}{z} + \left(1-\frac{1}{z}\right)\frac{(1-D-q_{+/+})\rho_+}{1-D-\rho_+}\right](1-D-q_{+/+})\right\}.
\end{aligned} \tag{8.10}$$

where ρ_+ is the global density of occupied $(+)$ patches, and $q_{+/+}$ the local densities defined as the conditional probabilities that a randomly chosen nearest neighbor of an occupied site is also occupied.

The internal equilibrium of the closed dynamical system given by Eqs. 8.11 with two variables ρ_+ and $q_{+/+}$ can be calculated by setting $d\rho_+/dt = 0$ and $dq_{+/+}/dt = 0$. A trivial solution given by $\hat{\rho}_+ = 0$ (extinction) always exists. In addition there is a non-zero equilibrium state, satisfying $0 < \hat{\rho_+} < 1$ and $0 \leq \hat{q}_{+/+} \leq 1$:

$$\hat{\rho}_+ = (1-D)\left[1 - \frac{e(z-1)}{zc(1-D) - c - e}\right], \qquad \hat{q}_{+/+} = 1 - D - e/c. \quad (8.11)$$

where the condition $D \leq 1 - e/c$ must be accomplished for $q_{+/+} \in \{0,1\}$. By explicitly assuming the effect of habitat loss *within* dispersal ranges Δ, the mean "effective" number of neighbors of a given empty patch z_{eff} is correctly rewritten as:

$$z_{eff} = z(1-D). \quad (8.12)$$

Then we get the close analytic expression for ρ_+:

$$\rho_+ = (1-D)\left[1 - \frac{e(z_{eff}-1)}{z_{eff}c(1-D) - c - e}\right] \quad (8.13)$$

These analytic results Eq. 8.11 and Eq. 8.13 allow us to test the improvements introduced by the pair approximation in predicting metapopulation patterns, with increasing habitat destruction. The analysis can be made considering the effects of habitat loss within dispersal ranges (Eq. 8.13) or not (Eq. 8.11). As shown in Fig. 8.4, the similarities between exact and approximated solutions (Eq.8.11 and Eq. 8.13) are remarkable. In particular, Fig. 8.4 shows that numerical simulations of the spatial model are always between the two limiting analytical curves obtained by the pair approximation method considering destruction within dispersal ranges (i.e., z_{eff}, Eq. 8.13) or not (i.e., z, Eq. 8.11). Depending on the value of z the simulation results fit better with one or the other pair approximated boundaries (see Fig. 8.4). In particular, as z values become larger, the dynamics is approximated better with Eq. 8.13 than with Eq. 8.11. In this sense, equilibrium dynamics of really local coupling (i.e., $z = 4$) does not need considering the effects of destruction at the local level. However, the contrary is true for the transient dynamics (pseudo-equilibrium patch occupancy values). As short-ranged dispersal (i.e., $z = 4$) usually involves large transient dynamics this result should also be taken into account. As it is observed in

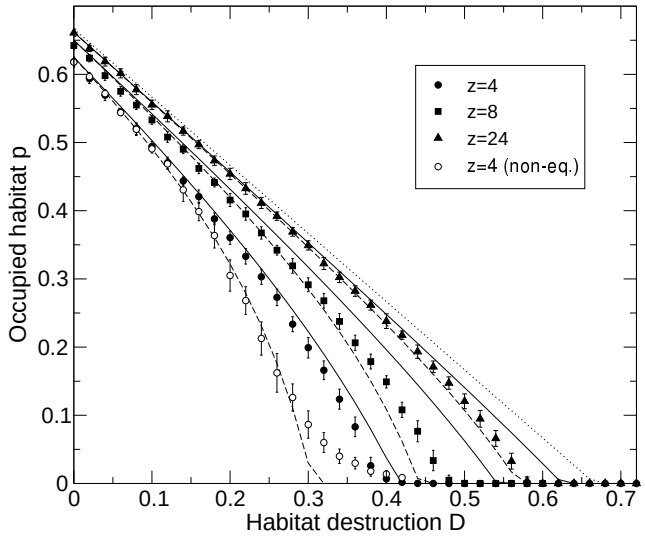

Figure 8.4: Numerical estimates of patch occupancy p in the spatially explicit model are plotted as functions of destroyed habitat D. Mean patch occupancy values (symbols) and variation (standard error bars) were obtained averaging over 25 realizations in a lattice of size 100×100. Parameters used: $c = 0.6$, and $e = 0.2$. All numerical simulations represent equilibrium scenarios 10^8 iterations, except one representing pseudo-equilibrium patch occupancy values (white circles, iterations 10^6). Broken lines represent the pair approximation predictions for $z = 4, 8$, and 24 assuming habitat loss effects within dispersal ranges z_{eff} (Eq. 8.11). Solid lines represent the pair approximation predictions for $z = 4, 8$, and 24, when not considering habitat loss effects within dispersal ranges z (Eq. 8.13). The dotted line represent the mean field solution for the Levins model with destruction, i.e., $p^* = 1 - D - e/c$.

Fig. 8.4 transient behavior for $z = 4$ is better fitted by the curve obtained from Eq. 8.13.

Thus, the pair approximation allows an adequate quantitative prediction of the equilibrium abundances and the extinction thresholds ($\rho_+ = 0$) for metapopulations in uncorrelated, destroyed habitats. These results allow us to calculate a relationship between extinction thresholds ($\rho_+ = 0$) and dispersal capacity z with some confidence. Thus, by making $\rho_+ = 0$ in Eq. 8.11, we can obtain an elegant analytical relationship between critical habitat destruction values (those destruction values that lead to metapopulation extinction), the dispersal capacity (expressed as z) and the metapopulation extinction (e) and colonization (c) rates, thus $D_c = f(z, e, c)$. The exact function obtained is:

$$D_c = 1 - \left(\frac{e}{c}\right) - \left(\frac{1}{z}\right). \tag{8.14}$$

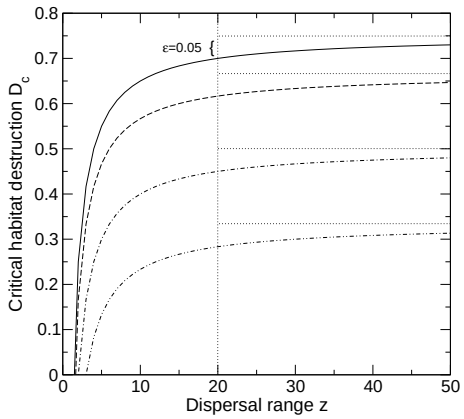

Figure 8.5: Relationship between the critical amount of habitat loss necessary for metapopulation persistence D_c and the dispersal range z obtained from equation 8.14. From top to bottom colonization (extinction) rates are 0.8(0.2), 0.6(0.2), 0.5(0.25), and 0.3(0.2). Horizontal dotted lines denote the corresponding mean field solutions $D_c = 1 - e/c$. At $z = 20$, divergence between mean field solutions and Eq. 8.14 solutions is equal to $\epsilon = 0.05$ (see text).

In Fig. 8.5 the behavior of Eq. 8.14 is shown. As z becomes larger the third term of the Eq. 8.14 becomes negligible, and D_c can be approximated by the solution of the mean field Levins model $D_c^{Levins} = 1 - e/c$. Indeed, the exact departure (i.e., ϵ) from the mean field solution due to dispersal z follows the power law:

$$\epsilon = [D_c^{Levins} - D_c] = \frac{1}{z}. \tag{8.15}$$

The hyperbolic approach to the mean field solution as z increases can be observed in Fig. 8.5. For $z > 20$ the discrepancy (error) between the mean field solution and Eq. 8.14 would be inferior to $\epsilon = 0.05$. Therefore, once defined a tolerance error ϵ, we can always define a *dispersal threshold* which would delimitate two differentiated dynamic regimes: Below the *dispersal threshold* the critical habitat destruction value for metapopulation to persist (D_c) is subjected to dispersal ranges. Beyond that, D_c and metapopulation persistence should mainly depend on colonization-extinction balances, therefore, metapopulation dynamics could be approximated by the Levins (mean field) model.

8.7 Discussion

Central to spatial spreading of populations is the concept of *contact kernel*, also known as *contact distribution* (Mollison, 1977) or *dispersal function* (Minogue, 1986): the probability distribution function for the displacement between the source and the point of deposition of a propagule. Based on empirical data, many models in population biology represent spatial dispersal as a local or exponentially-bounded process, using for example a negative-exponential or a step function of distance (Minogue & Fry, 1983; Zadocks & van den Bosch, 1984; Durrett & Levin, 1994; Filipe & Gibson, 1998). The recognition of an exponentially decaying *dispersal function* involves the existence of characteristic scales of dispersal (i.e., a mean and a maximum dispersal distance), and thus, a *dispersal range* (i.e., a set of potential colonization sites from a given disperser) can be defined.

There exists a high variability of dispersal distances among species, and among individuals of a given species, with a few individuals dispersing long distances relative to the median of the population (i.e., typically dispersal distance distributions have fat-tailed shapes, see Kot et al. (1996); Bullock et al. (2002)). Such rare long-distance dispersal events are difficult to observe but are important for the spread of species (Kot et al., 1996), as well as for preventing inbreeding in small populations (Mills & Allendorf, 1996). Simple models based on negative exponential dispersal functions, or similarly, on threshold dispersal ranges, while capturing the average behavior of the population of dispersers, significantly underestimate the potential for range expansion in many organisms (Kot et al., 1996). Therefore, the metapopulation model developed in the present study has heuristic value in estimating minimum thresholds of the likelihood that dispersing individuals (or species) can move particular distances between suitable habitats. However, it cannot be used to calculate directly the rates at which species could expand their ranges (i.e., spreading rates).

8.7.1 Dispersal and metapopulations

Within the metapopulation framework (Hanski et al., 1996; Hanski, 1998; Hanski & Gaggioti, 2004), dispersal has been considered the “glue” that keeps metapopulations together (Hansson, 1991; With & King, 2004), and thus is deemed crucial to metapopulation persistence. In reality, at any given scale, metapopulation connectivity (the density of such a glue, whether liquid or viscous (Pen, 2000)) depends on two interacting factors: landscape spatial structure and dispersal capacity.

When dispersal is rather limited the explicit topology of space becomes

more relevant. A lot of effort has been devoted to understand the effects of landscape spatial structure and patch network geometry for populations where dispersal is local (Dytham, 1994, 1995; Bascompte & Solé, 1996; Bascompte & Solé, 1998; Dieckmann et al., 2000). For example, the success of area-limited dispersal is enhanced on fractal landscapes due to the greater spatial contagion of habitat (With & King, 1999a). Also, the way suitable habitat is progressively lost has large effects on populations with strong dispersal constraints (Hiebeler, 2000; Ovaskainen et al., 2002). However, the spatial spreading of organisms is a powerful mechanism capable of modifying the spatiotemporal behavior of populations (Filipe & Maule, 2004; Law et al., 2003), which in turn, may screen landscape spatiotemporal patterns of habitat loss, fragmentation, or recovery. The interaction of both dynamics (i.e., landscape changes and population dispersal) should finally contribute (or not) to metapopulation's connectivity. The metapopulation capacity approach (Hanski & Ovaskainen, 2000; Ovaskainen & Hanski, 2001; Ovaskainen et al., 2002) integrates the effect of dispersal and spatial structure in a single pre-defined metapopulation connectivity metric. However, such an approach can be considered a mean field approximation in the sense that it ignores the part of spatial correlation that is generated by population dynamics (Ovaskainen et al., 2002). The effect of dispersal on metapopulation connectivity through population dynamics can only be analyzed by means of spatially explicit (lattice) models. In our simulations spatial heterogeneities emerge as a direct consequence of population dynamics and spatial spreading (i.e., extinctions, colonizations, and dispersal ranges). Specifically, we show that through specific dispersal ranges, the colonization dynamics of randomly located populations has direct consequences in the spatial structure of the metapopulation, modifying the long-term metapopulation connectivity and persistence. Other semi-analytic approaches may implicitly assume the existence of elements different from colonization-extinction dynamics (Bascompte, 2001).

8.7.2 Dispersal ranges and patch occupancy

The results of our study can be used to develop and assess potential solutions for problems involving habitat management and landscape planning. Managers must have knowledge of dispersal because it is a critical variable for modelling the effects of landscape change on the long-term viability of metapopulations (Beissinger & Westphal, 1998). The necessity of evaluating dispersal ranges (i.e., mean or maximum dispersal distances, home ranging, etc.) of endangered species to generate more accurate management and conservation policies becomes obvious when consider-

ing the fact that increasingly localized dispersal ranges shifts extinction thresholds to lower values of habitat loss (Fig. 8.4, Eqs. 8.11 and 8.13). For the same reason, the success of reintroductions of endangered species in fragmented habitats should greatly depend on the species characteristic dispersal range relative to suitable habitats inter-patch distances. Indeed, the major concerns about habitat fragmentation and landscape design are based in the ability of wildlife to disperse between blocks of habitat types that they require (Schumaker, 1996; Fahrig, 1997). Furthermore, the existence of a *dispersal threshold* could be relevant for managing purposes. Any empirical measure of dispersal capacity (i.e., mean dispersal distance, maximum dispersal range, dispersal area or domain, etc.) could be transformed into a value of z in a properly scaled spatially explicit model. Once made this transformation we could directly know, for the case under study, if the metapopulation is below or above the *dispersal threshold*, and thus, if metapopulation persistence estimates should be done by considering species dispersal capacities or not, respectively. If dispersal capacity is above the *dispersal threshold*) metapopulations' persistence and extinction thresholds become independent from dispersal mechanisms. Instead, they only depend on demographic metapopulation parameters. Note that the *dispersal threshold* is independent of the size of the landscape where the metapopulation survives, the key point is the scaling of the model in relation to real patch-neighboring distances.

Furthermore, our model also shows that beyond extinction, colonization and dispersal parameterization, the metapopulation persistence in a fragmented landscape depends strongly on "dynamical aspects". Depending on the dispersal capacity, the quantity of habitat lost *within* the dispersal range, and the dynamical status (i.e., whether equilibrium or not) of the metapopulation, habitat loss can have an *added* negative effect on metapopulation persistence. For poor dispersers (i.e., dispersal limited to nearest neighbors) extinction thresholds are low, but the clumped spatial structures generated by short-ranged dispersal strategies prevent them from being even lower. In such cases, the metapopulation is "protected" (at the long-term limit and only to some extent) from *added* negative effects due to a dynamical decrease in colonization rates. In these cases, the effects of habitat loss *within* dispersal ranges are important only during transient dynamics but not for the long-term equilibrium dynamics. In metapopulations with long-range dispersal strategies species extinction thresholds are higher. However, the fraction of habitat lost *within* dispersal ranges is larger, ensuring permanent *added* negative dynamical effects on colonization rates. In these cases, landscape habitat destruction effectively decreases the mean number of potential colonizers within the dis-

persal ranges, providing an effective decrease of long-term metapopulation persistence. For intermediate dispersal ranges we may expect intermediate dynamical effects. The long-term metapopulation persistence will be obtained as a dynamical trade-off between the *added* positive effects of a clumped-like colonization process, and the *added* negative effects of long-ranged dispersal. Fig. 8.4 shows these dynamical effects on metapopulation persistence. It is observed that for $z = 4$ (i.e., short-ranged dispersal) the spatially explicit simulation equilibrium-results fit better with the pair approximation without considering habitat loss *within* dispersal ranges. On the contrary, when transient or pseudo-equilibrium patch occupancy is considered, this effect is important. For $z = 8$, the simulation results are just between both analytical curves. And finally, for $z = 24$ (i.e., long-ranged dispersal) simulation results fit better with the curve obtained from Eq. 8.13 (when no destruction is considered *within* dispersal ranges). The utilization of both possible solutions, Eq. 8.11 and Eq. 8.13 allow us to approximate better the spatiotemporal dynamics of the metapopulation involving both transient and equilibrium states. Whenever uncorrelated destruction assumption is possible, the area within both analytical curves may provide an adequate interval estimate of real extinction thresholds. In non-random fragmented habitats, deviations from such a null model may help to understand potential effects of landscape's spatial configurations to metapopulation connectivity and persistence.

8.7.3 Dispersal ranges and transient times

The transient time, the time it takes for a population to return to population-dynamic equilibrium following a perturbation in the environment or in population size, shows a divergent behavior near the extinction threshold (i.e., when a critical habitat destruction value D_c is reached, see 8.2b). Our analytical approach for both the time to reach equilibrium values ($D \leq D_c$, Eq. 8.6), and the time to extinction ($D > D_c$, Eq. 8.7) is directly derived from considering the Levins model a logistic-growth model. Different approaches (not so straightforward) have lead to the same result: that the transient time is expected to be longer for those species for which perturbed environment is close to the threshold of persistence, suggesting that species extinction due to habitat loss may take a long time (Ovaskainen & Hanski, 2002). As stated in Hanski & Ovaskainen (2002) this result is specially noteworthy for conservation biology because extinction threat is likely to be underestimated in changing environments in exactly those cases where it matters most.

A new question to be addressed in relation to transient times is: What is

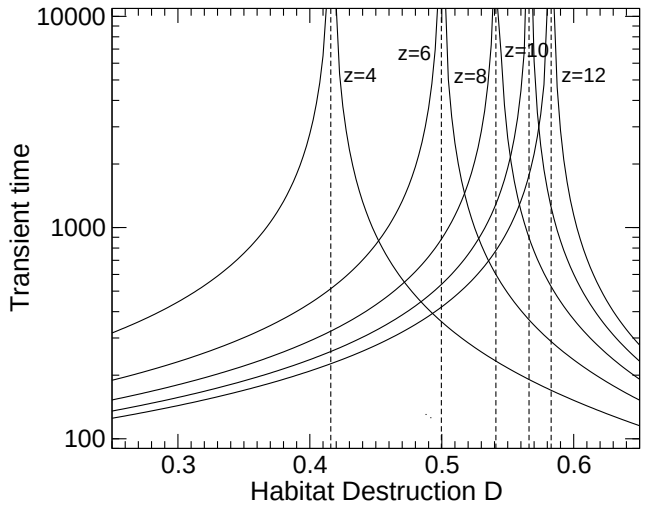

Figure 8.6: Transient time behavior for different dispersal capacities z in relation to habitat destruction D. The results are obtained from numerical integration of the pair approximation system of equations (Eq. 8.11) by Runge-Kutta (order 8) method. Parameters: extinction rate $e = 0.2$, colonization rate $c = 0.6$, initial population fraction $p_0 = 0.9999$, and $\eta = 0.9999$ considered a small perturbation from the steady state computed with equation 8.11.

the effect of dispersal ranging on transient time metapopulation behaviors? Figure 8.6 shows the transient time behavior of the equation system 8.11 in relation to habitat destruction for different dispersal capacities.

Three results can be highlighted from Fig. 8.6. First, the divergence observed for the transient time near the extinction threshold in the mean field model (Fig. 8.3d) is also observed when dispersal capacity is explicitly included (Fig. 8.6). Therefore, for any dispersal range z, transient times near extinction thresholds become infinitely large ($T \to \infty$). Close to such critical points we should expect correlations scaling with the system following well-defined power laws (Solé et al., 1999). Second, far from extinction thresholds and in $D < D_c$ regimes, shorter dispersal ranges involve larger transient times. While the contrary is true for $D > D_c$ regimes. Thus, dispersal capacity makes transitory dynamics shorter in order to reach non-zero equilibrium values, and larger when the equilibrium solution is the extinction. And third, given a specific amount of destroyed habitat, dispersal capacity is a key element to decide whether a species is prone to go extinct or to survive. From these results, it is derived that when evaluating the extinction debt accumulated in a given species community (Tilman et al., 1994; Hanski & Ovaskainen, 2002) dispersal capacity should be taken into

account. The demographic metapopulation parameters and the degree of habitat destruction are not enough to positioning the community extinction thresholds. For example, for $D = 0.45$ in Fig. 8.6 a species with the same colonization-extinction parameters ($e = 0.2, c = 0.6$) should be included in the extinction debt list if its dispersal range is $z = 4$, but it should not be included if dispersal range is $z = 6$. In this concrete case, transient times to reach both equilibriums (extinction and non-zero respectively) is exactly the same. Finally, in highly destroyed habitats ($D > D_c$ regimes) it should be taken into account that, given similar demographic parameters for the community, those species with large-range dispersal are more prone to be technically extinct (thus, inflating the extinction debt list) than short-ranged species. This is so, because for species with large-range dispersal strategies, transient times to extinction are larger. Overall, we should be aware that, besides the fact that finite-size effects can lead to slow stochastic extinction of species (Solé & Goodwin, 2000; McKane et al., 2000; Hubbell, 2001), dispersal range effects could also be increasing the number of species in the extinction debt list.

8.7.4 Model extensions

The new mathematical expression for the Levins model (Eq. 8.11) has the added value of useful closed-form analytical solutions. Equation 8.14, for example, should enable us to make reasonable risk assessments of extinction thresholds based on dispersal characteristics. Finally, it should be noted that with an appropriate interpretation of the dispersal range parameter z, our analytical results could also be valid in spatially realistic metapopulation approaches. If possible, these equations could be interpreted as the spatially explicit analytical counterpart of the metapopulation capacity approach (Hanski & Ovaskainen, 2000).

One particularly relevant extension of this approach is to consider a complex landscape formed by many, perhaps heterogeneous patches. Specifically, the situation is described by a network defined as a set of nodes (patches of landscape) coupled through dispersal. Here two nodes are linked if a given species is able to move from one to the other. If the dispersal range of such species is η, then the presence of a link is

$$A_{ij} = \begin{cases} 1 & \text{if } \left\| S_i - S_j \right\| < \eta \\ 0 & \text{otherwise} \end{cases}$$

The matrix A_{ij} defines the overall architecture of the lanscape network, as seen by the species under consideration.

A generalized Levins-like model of such network would be defined as a set of N coupled equations. Now if the degree distribution associated to the set of patches is indicated as $P(k)$, an average number of links per patch can be defined as

$$\langle z \rangle = \sum_{k=1}^{N} kP(k)$$

where $P(k)$ is the probability of a given patch to have k links. Given the local nature of the patch-patch relationship, we sould expect $P(k)$ to be a Poisson-like distribution. In that case, we could replace z in the previous models by $\langle z \rangle$. If $P(k)$ is not so homogeneous, then analytic approximation to the full set of equations sould be taken (Pastor-Satorras & Vespigniani, 2001).

Acknowledgments

F.B acknowledges David Alonso for his help in the implementation of the stochastic spatial explicit Levins model, and Andreea Munteanu for help in the understanding of the work developed by D. Gillespie in relation to chemical reaction exact stochastic simulations.

8.8 Appendix

8.8.1 Analytical solutions for transient dynamics

Exact solution for non-null near-steady states: $D \leq D_c$

We start the calculation of the time it takes for a population to reach a population-dynamic equilibrium by noting that the Levins metapopulation model Eq. 8.1 is identical with the logistic population growth model given as:

$$\frac{dp}{dt} = ap - cp^2. \tag{8.16}$$

where $a = c\Gamma$ and $\Gamma = 1 - D - e/c$.
This is a separable differential equation that can be rewritten as,

$$\int_{p_0}^{p} \frac{dr}{ar - cr^2} = \int_{t_0}^{t} ds = t - t_0. \tag{8.17}$$

To integrate the function $1/(ar - br^2)$ we resort to partial fractions and obtain.

$$\int_{p_0}^{p} \frac{dr}{r(a-cr)} = \frac{1}{a}\int_{p_0}^{p}\left(\frac{1}{r} + \frac{b}{a-cr}\right)dr = \tag{8.18}$$

$$= \frac{1}{a}\left[\ln\frac{p}{p_0} + \ln\left|\frac{a-cp_0}{a-cp}\right|\right] = \frac{1}{a}\ln\frac{p}{p_0}\left|\frac{a-cp_0}{a-cp}\right|. \tag{8.19}$$

Thus,

$$a(t-t_0) = \ln\frac{p}{p_0}\left|\frac{a-cp_0}{a-cp}\right|. \tag{8.20}$$

It can be easily shown that $(a-cp_0)/(a-cp(t))$ is always positive for $p_0 < p$ and hence,

$$a(t-t_0) = \ln\frac{p}{p_0}\left(\frac{a-cp_0}{a-cp}\right). \tag{8.21}$$

For $t_0 = 0$ we have,

$$t = \frac{1}{a}\ln\frac{p}{p_0}\left(\frac{a-cp_0}{a-cp}\right). \tag{8.22}$$

Making the appropriate change in the variables for the Levins model where $a = c\Gamma$ we obtain,

$$T = \frac{1}{c\Gamma}\ln\frac{p}{p_0}\left(\frac{\Gamma-p_0}{\Gamma-p}\right). \tag{8.23}$$

where $\Gamma = 1 - D - e/c$. If $p = \Gamma - \eta$ where $\eta \ll \Gamma$, then,

$$T(D,\eta) = \frac{1}{c\Gamma}\ln\left[\frac{\Gamma-\eta}{p_0}\left(\frac{\Gamma-p_0}{\eta}\right)\right] \tag{8.24}$$

As $T(D,\eta)$ must be always positive, this equation is only valid for $p > p_0 \equiv \Gamma > p_0$, that is, only when $D \leq D_c$ (i.e., a non-trivial stable equilibrium population value).

Approximated solution for time to extinction: $D > D_c$

Starting from an initial condition $p_0 \ll 1$ and assuming $D > D_c$ we always will obtain decayment until reaching extinction. Levins equation,

$$\frac{dp}{dt} = cp(1-D-p) - ep = \Omega p - cp^2. \tag{8.25}$$

where $\Omega = c(1-D) - e$ will be dominated only by the first term, because $p_0 \ll 1$. Thus, we have

$$\left(\frac{dp}{dt}\right)_{D>D_c} \approx \Omega p \tag{8.26}$$

The time required to reach a fraction of the steady population $0 \leq \eta \ll 1$ and $\eta < p_0$ can be computed by rewriting equation 8.26 as follows,

$$\int_{p_0}^{\eta} \frac{dp}{p} = \Omega \int_{t_0}^{T} dt. \tag{8.27}$$

Therefore,

$$\ln\left(\frac{\eta}{p_0}\right) = \Omega T. \tag{8.28}$$

and

$$T(D,\eta) = \frac{1}{\Omega} \ln\left(\frac{\eta}{p_0}\right). \tag{8.29}$$

for $D > D_C$ and $\Omega = c(1-D) - e$.

8.8.2 The exact stochastic algorithm for the spatially explicit Levins model

The fundamentals of the *exact stochastic algorithm* were developed in the context of chemical coupled reaction systems (Gillespie, 1976, 1977, 1992). Simple applications to birth-rate processes are described in Renshaw (1991). More recently, the exact stochastic algorithm has been generalized to be used in discrete spatially extended systems (Alonso & McKane, 2002; Alonso, 2003). The simulation procedure is a bit different from the one described in Gillespie (1976, 1977, 1992). The spatially extended version of the algorithm includes the *rejection method* (Press et al., 1992) which enables a rapid random election of different possible site or patch events according to their rates, in particular, when these different rates take comparable values. Indeed, in spatially extended models the stochastic algorithm involve a three step process decision: i) When will occur the next event?, ii) Where will occur the next event?, and iii) Which will be the next event?. In non-spatial models, the stochastic algorithm only must account for the questions i and iii. The common point in any exact stochastic simulation strategy is the computation of a total transition rate for the whole system which is then used to estimate inter-events time, determining when it will take place the next event.

Here, we will only describe the specific algorithm used for performing exact stochastic realizations of the spatially explicit (lattice) Levins model. For a more general view see Alonso & McKane (2002); Alonso (2003).

We must start remembering the basic assumptions underlying the Levins spatially explicit model: i) patches are distributed uniformly in a

two-dimensional lattice of $N \times N$ sites, ii) Patch dynamics involve two transition events: extinction and colonization, iii) Given a certain configuration of the system, the basic dynamical processes underlying patches (i.e., patch transition rates) depend on the state of the patch (whether occupied [+] or available [0]), and the state of the neighboring patches.

The patch transition events can be illustrated as follows:

$$\text{Occupied patches – Extinction: } [+] \xrightarrow{e} [0] \tag{8.30}$$

$$\text{Available patches – Colonization: } [+,0] \xrightarrow{c/z} [+,+] \tag{8.31}$$

Each patch in the lattice can be extinct at a constant rate e (i.e., extinction rate is the same for all the patches, this it is global). Instead, the colonization rate of an empty patch depends on a neighborhood domain of occupied patches. The neighborhood domain $Z(p)$ symbolizes the dispersal range. The size of the dispersal range is given in terms of the number of neighbors z to be considered for a given patch. The colonization rate per *each* neighboring patch is defined as c/z. Indeed, the colonization rate c, is the maximum colonization rate into an empty patch, which is realized when all the neighbors in the dispersal range are occupied. Therefore, an empty site will be filled by a local population at a rate proportional to the number of occupied neighbors in the dispersal range.

The following definitions of *neighborhood colonization pressures* will be needed in the stochastic algorithm:

- *Colonization pressure of neighboring patches within $Z(p)$ to an empty central patch $p = x$.* By definition patch x must be available $x = p_0 = 0$

$$c(Z)_x = \frac{c}{z} \sum_{p \in Z(p)} p_+. \tag{8.32}$$

  Colonization pressure of a central patch $p = x$ on empty neighboring patches within $Z(p)$. By definition patch x must be occupied $x = p_+ = 1$.

$$c(x)_Z = \frac{c}{z} \sum_{p \in Z(p)} (1 - p_+). \tag{8.33}$$

where p_+ is the number of occupied patches, $(1 - p_+) = p_0$ the number of available patches, and z is the maximum number of neighbors in the dispersal range $Z(p)$. Note that if habitat fragmentation is included (and landscape dynamics is not taken into account), the destroyed patches are not involved in patch dynamics, thus they need not to be considered in any of these calculations.

The overview of the algorithm is as follows:

1. Calculation of the *total transition rate* of the system R. This is the probability per unit time that the system changes configuration as a result of a transition event occurring in any patch within the system.

2. Calculation of the *expected time to next transition* t.

3. *Rejection method.* Choose a patch at random and assess whether this patch will undergo a transition or not. If not, stochastic time is assumed not to advance and nothing happens. If it can, the inter-event expected time calculated in the previous step is accumulated and a particular transition event (compatible with the chosen patch) takes place changing the configuration of the system.

4. Repeat again starting from step 1.

Here we describe in detail the three main steps enumerated above:

Total transition rate: Sum up all the event transition rates of the system at time t. This can be done by computing the number of occupied sites n_+ and the number of available sites surrounded with a given number i of occupied neighbors n_{0i}, where $i = 1,..,z$ and $\sum_{i=0}^{z} n_{0i} = n_0$, where n_0 is the number of available sites. Thus, in the first iteration of the simulation we have to compute,

$$R = en_1 + \sum_{i=0}^{z} c\left(\frac{i}{z}\right) n_{0i} \tag{8.34}$$

Inter-event expected time: The expected time to next transition t can be estimated by sampling an exponential distribution with parameter R,

$$t = \frac{-\log(\chi)}{R} \tag{8.35}$$

where χ is a uniformly distributed random variable (Gillespie, 1976, 1977; Renshaw, 1991; Gillespie, 1992) (see also Technical Appendix A). Thus, in this way we are actually sampling this distribution and estimating "when will occur the next event". Accumulating these inter-event times for every stochastic realization we are able to correctly track the time.

Rejection method: The rejection method allow us to know "where will occur the next event " and "which event will occur". The basic idea is based on the fact that at each time step we have a different configuration of patch-states in the lattice. Thus, at each time step, patch transition rates r should change accordingly. These transition rates depend not only on patch states, but also on the neighboring patch states within the dispersal range $Z(p)$. If a patch is occupied, the patch-rate for that patch, is simply e. If available

the patch-rate must be computed as $c(\frac{i}{z})$, where i is the number of occupied neighbors in the dispersal range, and z the number of total neighbors in the dispersal range.

Thus, at each time step, we can define a discrete two-dimensional probability distribution of transition rates emerging from the whole $N \times N$ patch-lattice system. The rejection method allow us to randomly sample patches or site according to this distribution. First we need to normalize these patch-transition rates by the *maximum patch-rate* r_{max} in the system. Depending on the system configuration r_{max} can be either related to an extinction event or to the colonization event with the largest number of occupied neighbors.

Then we can apply the rejection method in the following way:

- Choose a patch at random $k - patch$.
- Compute the following ratio: $x = r_k / r_{max}$
- Compare x value to a randomly chosen number, χ, belonging to a uniform distribution lying between 0 and 1. If $\chi < x$ this patch is accepted and undergoes a transition regarding to its state (whether an extinction or a colonization). If not, the patch is rejected and the rejection procedure is repeated.
- Once a patch is accepted, we can directly know "what event will happen" in relation to its state. If the selected patch is one available, the transition event will be a colonization. If occupied, the transition event will be an extinction.

To carry out this procedure in the most efficient manner, at the initial simulation step t_0, we should store: First the n_+ and n_{0i} values to compute R. The occupied patches can be stored in a scalar variable. The available sites may be stored in a vector $\vec{n_0} = 0, 1, ..., z$, where all available patches with 0 occupied neighbors will be stored at $n_0[0]$, those with 1 occupied neighbor at $n_0[1]$, ..., and those with all the neighbors occupied at $n_0[z]$. Second, the maximum patch-rate r_{max}. Depending on the system configuration r_{max} can be either related to an extinction event or to a colonization event.

Then, in the course of updating the parameter R after the occurrence of each transition event, we need only to substract or add the new values obtained from the "neighborhood colonization pressures" calculations in the following way:

$$\text{Extinction of x: } [+] \longrightarrow [0] : R_1 = R_0 + c(Z)_x - c(x)_Z \tag{8.36}$$

$$\text{Colonization of x: } [0] \longrightarrow [+] : R_1 = R_0 - c(Z)_x + c(x)_Z \tag{8.37}$$

where R_0 is the total transition rate at time step t_0 and R_1 at time step $t_1 = t_0 + 1$. Then, we need to update the value n_+ and the vector n_{0i} by adding or subtracting a unit value accordingly with the transition event occurred: extinction or colonization. In the latter case, we must know which is the number of occupied neighbors involved in that specific colonization to update the vector $\vec{n_0}$ correctly). If we are not interested in characterizing the evolution on time of available sites in relation to their neighborhood occupancy the vector $\vec{n_0}$ need not to be actualized. Finally, we need to update r_{max}. This can be done, by comparing the previous r_{max} to the specific transition rate event of the selected patch r_k. If $r_k > r_max$ then $r_max = r_k$, else $r_max = r_max$.

Pseudo-code

Initialization

1. Initialize parameter values for colonization c and extinction e rates. Initialize habitat destruction percentage value D.
2. Initialize lattice configuration (i.e., random placement of occupied, available and destroyed patches).
3. Compute n_+, n_{0i}, R and r_{max}.
4. Set $t = 0$

Main Loop

1. Randomly select a patch in the lattice. Generate a discrete uniformly distributed random number between 0 and $N \times N$ (irand).
2. Decide whether the selected patch will undergo a transition. Generate a continuous uniformly distributed random number (drand):

   If $r/r_{max} >$ drand $\rightarrow$ NO EVENT. Start at step 1 Main Loop again.

   If $r/r_{max} <$ drand $\rightarrow$ EVENT. Continue to next step.
3. Compute *neighborhood colonization pressures* of the selected patch: $c(Z)_x$ and $c(x)_Z$.
4. Generate a continuous uniformly distributed random number (drand2) and get an inter-event time $\tau = -\ln(\text{drand2})/R$.
5. Actualize R and r_max according to the transition occurred.
6. Do $t = t + \tau$.
7. Return to step 1 in Main Loop.

8.8.3 The pair approximation method

As shown in Appendix A.1, the classical Levins model is in fact a logistic equation. Therefore, its spatially explicit version can be considered a "lattice logistic model", also referred as the "basic contact process" (Mollison, 1977). The development of the pair approximation method for a lattice basic contact process is described in detail in Sato & Iwasa (2000). We have introduced the habitat destruction effect in the model worked out in Sato & Iwasa (2000) and followed their analytical development.

The model described (see Section 8.4) assumes the existence of a dispersal range Δ to describe the dynamics of metapopulation densities (fraction of occupied or available sites in the lattice). In particular, the colonization rate depends on the number of occupied neighbors in the dispersal range of a randomly chosen available site rather than on the overall average occupancy of the lattice. Thus, it is difficult to construct a simple model of population dynamics as an ordinary differential equation based only on the overall density of the metapopulation. Instead, it is necessary to distinguish between global (whether singlet or doublet) densities and local (or conditioned) densities (Matsuda et al., 1992). The state of a site is denoted by σ, which is either + (occupied) or 0 (available). Global singlet-densities ρ_σ, with $\sigma \in \{+, 0\}$, are the probabilities that a randomly chosen lattice site is in state σ. Local densities $q_{\sigma/\sigma'}$, with $\sigma, \sigma' \in \{+, 0\}$, are the conditional probabilities that a randomly chosen nearest neighbor of a site in state σ' is in state σ. The difference between ρ_σ and $q_{\sigma/\sigma'}$, indicates nearest-neighbor correlation. These local densities can be expressed in terms of global doublet-densities $\rho_{\sigma\sigma'}$, which are the probabilities that a randomly chosen pair of nearest-neighbor sites are in state $\sigma\sigma'$. Doublet densities can be expressed as the products of singlet densities and local densities:$\rho_{\sigma\sigma'} = \rho_{\sigma'\sigma} = \rho_\sigma q_{\sigma'/\sigma} = \rho'_\sigma q_{\sigma/\sigma'}$. Higher-order densities, such as triplet or quartet densities, can be defined similarly. By definition, global and local densities satisfy

$$\begin{aligned} \sum_{\sigma\in\{+,0\}} \rho_\sigma &= 1 \\ \sum_{\sigma\in\{+,0\}} q_{\sigma/\sigma'} &= 1, \qquad \forall\ \sigma' \in \{+, 0\}. \end{aligned} \tag{8.38}$$

As the initial configuration is uniformly distributed and the processes are spatially homogeneous and isotropic, the probabilities ρ_σ and $\rho_{\sigma\sigma'}$ remain independent of location. These probabilities change over time t. According to processes 8.30 and 8.31, global density develops over time as follows:

$$\frac{d\rho_+}{dt} = -e\rho_+ + c(q_{0/+})\rho_+. \tag{8.39}$$

The first and second terms on the right-hand side of the equation correspond to the extinction and colonization processes, respectively. The second term includes the local average density of occupied sites adjacent to available sites $q_{0/+}$. As we do not assume any assimetry between neighboring sites $q_{0/+} = q_{+/0} = 1 - q_{+/+}$. When habitat destruction D is considered, we obtain the following expression $q_{0/+} = 1 - D - q_{+/+}$.
The doublet density changes according to the dynamics

$$\frac{d\rho_{++}}{dt} = -2e\rho_{++} + 2\frac{c}{z}\rho_{+0} + 2\frac{c}{z}(z-1)q_{+/0+}\rho_{+0}. \tag{8.40}$$

This equation includes the extinction term (the first term on the right-hand side) and the colonization terms (the second and third terms). The first term describes transitions of pairs in state ++ to either 0+ or +0. Both transitions occur at a rate e and thus give rise to the factor $2e$. In the second and the third terms of the equation, the factor 2 is needed because we do not assume any assimetry in the interaction between sites, which means $\rho_{+0} = \rho_{0+}$. So we have to include both transitions from 0+ and +0 to ++. The second term indicates the case where + occupies the nearest-neighbor 0 site within the pair. The third term correspond to events in which an empty site of a pair becomes occupied by another neighbor (which is not part of the pair). Thus, in two-dimensional square lattice and $z = 4$ we must consider three sites (in general $z - 1$ sites) in the dynamics of local densities. This approach neglect differences in the spatial configuration of these three connected sites on the two-dimensional square lattice.
Eq. 8.40 is incomplete without knowledge of $q_{+/0+}$. To overcome this difficulty, we adopt an approximation, called the decoupling method (or moment closure), which neglects higher-order correlations (triplet or quartet densities). Thus, the method is named pair approximation because it traces pair correlations but neglect three-site correlations (Matsuda et al., 1992; Sato et al., 1994). Pair approximations focus only on the nearest-neighbor correlation; correlations between non-nearest neighbors are approximately reconstructed from nearest-neighbor correlations. In general, $q_{\sigma/\sigma'\sigma''}$ is replaced by $q_{\sigma/\sigma'}$. Underlying this assumption is the idea that the correlation between lattice sites decreases monotonically with the distance between them. Thus a site is affected less by distant neighbors than by intermediate neighbors. The higher-order conditional probabilities in Eq. 8.40 thus can be reduced as follows:

$$q_{+/0+} \approx q_{+/0} = \frac{\rho_{+0}}{\rho_0} = \frac{(1 - D - q_{+/+})\rho_+}{1 - \rho_+}. \tag{8.41}$$

Because doublet densities are the products of global and local densities, we can express the local densities as the ratio of doublet densities to singlet

(global) densities. Hence the dynamics of local density can be written as follows:

$$\frac{dq_{+/+}}{dt} = \frac{d(\rho_{++}/\rho_{+})}{dt}. \tag{8.42}$$

Such a function $d/dt\phi(\rho_{++},\rho_{+})$ can be expressed in terms of its partial derivatives by following the *chain rule*:

$$\frac{d}{dt}\phi(\rho_{+},\rho_{++}) = \frac{\partial\phi}{\partial\rho_{+}}\left(\frac{\partial\rho_{+}}{dt}\right) + \frac{\partial\phi}{\partial\rho_{++}}\left(\frac{d\rho_{++}}{dt}\right). \tag{8.43}$$

So we have

$$\begin{aligned}\frac{d(\rho_{+}/\rho_{++})}{dt} &= \frac{\partial\left(\frac{\rho_{++}}{\rho_{+}}\right)}{\partial\rho_{+}}\frac{d\rho_{+}}{dt} + \frac{\partial\left(\frac{\rho_{++}}{\rho_{+}}\right)}{\partial\rho_{++}}\frac{d\rho_{++}}{dt} \\ &= \rho_{++}\frac{\partial}{\partial\rho_{+}}\left(\frac{1}{\rho_{+}}\right)\frac{d\rho_{+}}{dt} + \frac{1}{\rho_{+}}\frac{d\rho_{++}}{dt}.\end{aligned} \tag{8.44}$$

And therefore,

$$\frac{dq_{+/+}}{dt} = \frac{d(\rho_{++}/\rho_{+})}{dt} = -\frac{\rho_{++}}{\rho_{+}^{2}}\frac{d\rho_{+}}{dt} + \frac{1}{\rho_{+}}\frac{d\rho_{++}}{dt}. \tag{8.45}$$

Finally, considering the following expressions:

$\rho_{++} = \rho_{+}q_{+/+}$.
$\rho_{+0} = (1 - D - q_{+/+})\rho_{+}$.
$q_{+/0+} \approx q_{+/0} = \frac{\rho_{+0}}{\rho_{0}} = \frac{(1-D-q_{+/+})\rho_{+}}{1-\rho_{+}}$.

and substituting Eq. 8.40 into Eq. 8.45, we obtain the following expression for the local densities:

$$\begin{aligned}&\frac{dq_{+/+}}{dt} = -q_{+/+}[c(1 - D - q_{+/+}) - e] + \\ &+2\left\{-eq_{+/+} + c\left[\frac{1}{z} + \left(1 - \frac{1}{z}\right)\frac{(1 - D - q_{+/+})\rho_{+}}{1 - D - \rho_{+}}\right](1 - D - q_{+/+})\right\}.\end{aligned}$$

So we obtain the following set of equations from Eq. 8.39 and Eq. 8.45:

$$\begin{aligned}&\frac{d\rho_{+}}{dt} = -e\rho_{+} + c(1 - D - q_{+/+})\rho_{+} \\ &\frac{dq_{+/+}}{dt} = -q_{+/+}[c(1 - D - q_{+/+}) - e] + \\ &+2\left\{-eq_{+/+} + c\left[\frac{1}{z} + \left(1 - \frac{1}{z}\right)\frac{(1 - D - q_{+/+})\rho_{+}}{1 - D - \rho_{+}}\right](1 - D - q_{+/+})\right\}.\end{aligned} \tag{8.46}$$

Thus, with the pair approximation method we can express the Levins spatially explicit model with habitat destruction and dispersal ranges in terms of a closed dynamical system (Eq. 8.46) with two variables ρ_+ and $q_{+/+}$, global occupancy densities and local densities (nearest-neighbors occupancy correlations).